140

THE DAMAGE EFFECTS OF HIGH ENERGY RADIATION ON LITHIUM FLUORIDE THERMOLUMINESCENT DOSIMETERS

A Thesis

Submitted to the Graduate Faculty of the
Louisiana State University and
Agricultural and Mechanical College
in partial fulfillment of the
requirements for the degree of
Master of Sciences

in

The Department of Nuclear Engineering

by
William Wade Ballard, Jr.
B.S., Louisiana State University, 1967
August, 1968

ACKNOWLEDGEMENTS

The author is indebted to Dr. Robert C. McIlhenny of the Louisiana State University Nuclear Science Center for directing this research and serving as major advisor. His guidance, encouragement, and diligence are truly appreciated.

A special thanks to Mr. Marshall Parrot of the Tulane University Primate Center for making this research possible through the loan of the necessary apparatus; and Dr. Frank Iddings for making available the facilities of Accelerators Inc.

Finally the author would like to acknowledge Miss Kay Thomas who deserves special consideration for her excellent typing of this manuscript.

TABLE OF CONTENTS

LIST OF FIGURES

ABSTRACT

The damaging effect of high energy radiation was studied for lithium fluoride thermoluminescent dosimeters. The virgin LiF powder was first annealed at 400°C for one hour followed by an 80°C annealing for 24 hours. Samples weighing 35 mg. were exposed to damaging doses of ^{60}Co ranging from 10^3 to 10^8 R, followed by a similar annealing. The damaged dosimeters were then exposed to a uniform dose of 10^3 R and the thermoluminescent response recorded. The exposure-annealing cycle was then repeated for 500°C and 600°C annealings. By defining $R_D = S_v/S_D$ as the relative response with respect to undamaged dosimeters it is experimentally shown that

$$(R_D-1) = P\ (1-e^{-k_1 D}) + P\ (1-e^{-k_2 D}) + P\ (1-e^{-k_3 D})$$

where k_1, k_2, and k_3 are characteristic trapping probabilities and P_1, P_2, and P_3 vary with annealing temperatures. The three terms are assumed to be three different types of non-radiative traps created by the massive radiation doses.

Assuming all metastable traps are either radiative or non-radiative, and only non-radiative traps are created by the damage doses, it is shown that the fraction of radiative traps decrease with increasing doses. By representing this competing reaction as first order kinetics it is shown that the relative response is of the form

$$(R_D-1) = \sum_{i=1}^{n} [\ P_i(1-e^{-k_i D})]$$

By assuming n=3, a correlation can be made between the theoretical development and experimental data.

INTRODUCTION

Statement of Problem

In the development of the thermoluminescent phenomena many interesting characteristics have been observed, some of which cannot be explained from existing literature. If the expectations of these dosimeters are to be fulfilled therefore, it becomes necessary to examine the aspects which may influence their performance, and to explain deviations from the most consistant literature available. The most prevalent applications seem to be oriented into three realms of science: in-vivo dose measurements in the medical field, dose determination where the dosimeter size is the limiting factor, and personnel monitoring. The two characteristics which cause this wide diversification for applications of TLD are its ability to duplicate the dose equivalent of human tissue and its approximity to a point detector. To broaden this spectrum of uses even more a deeper insight as to the fundamental mechanisms of thermoluminescence should be achieved. In fact, the published literature available seems to suggest that the exact type of defect causing thermoluminescence has not been isolated. To approach this problem, a worthwhile venture would appear to be an investigation into the effects of massive doses of radiation on the thermoluminescent response. By varying doses and types of radiation, some sort of hypothesis should make itself apparent.

Marrone and Attix [1] first observed that permanent damage in the gamma ray responsiveness of LiF phosphors occurred for exposures of the order of 10^4 roentgens. Two years later, Doppke and Cameron [2] obtained similar results and attempted to explain their data from the standpoint of electron theory.

The investigation of fast neutron damage was not reported until early 1967, when Oltman, Kastner, Tedeschi, and Beggs [3] published the results of their experiments using 4.0 MeV neutrons from a Van de Graff accelerator.

The experimental gap then would appear to be some sort of correlation between dose and damage for both neutrons and gamma radiation. By maintaining close control of the variables involved, the results of such a comparison should give some indication as to the mechanisms involved in the damage. Such is the purpose of this thesis.

Theory

Interactions of Radiation With Matter [4] [5] [6]

In this discussion the study of gamma rays and neutrons will be of prime importance. This is not to ignore the effects of charged particles, because in the final analysis there is a connection between the two. Neutrons may cause transmutation, leading to the emission of radiation as a result of the interaction and afterwards as decay radiation. In addition, direct elastic collisions by gamma rays and neutrons with electrons and nuclei produce high speed charged particles. Therefore to study neutral radiation necessarily involves charged particles.

The interaction of high energy photons with solids usually occurs as one of three possibilities: photoelectric effect, Compton scatter, or pair production. The probability of an isolated photon causing any one of these interactions is a function of the energy of the photon, and can be expressed as a probability cross section. The sum of these cross sections, σc, σp, and σpp, is usually referred to as the attenuation coefficient, μ. In the photoelectric effect the incoming photon collides with and expels an inner orbital electron with energy P, where P is the difference between the photon energy and the binding energy of the electron. The probability cross section for this case can be expressed as

$$\sigma p = K \frac{Z^n}{E^k} \qquad (1\text{-}1)$$

where: (1) K varies from 3 to 1 for photon energies from 10 KeV to several MeV

(2) n varies from 4 to 4.6 for photon energies from 0.1 to 3 MeV

(3) E is the initial photon energy

(4) Z is the atomic number of the affected atom

In Compton scatter, a photon makes an elastic collision with a valence electron, resulting in a deflected photon with less energy. In the collision both momentum and energy are conserved, and part of the energy of the incident photon is transferred to the electron. The relation between the energy E of the incident photon, E' of the scattered photon, and the scattering angle θ, is given by

$$E' = \frac{0.51}{(1-\cos\theta) + (0.51/E)} \qquad (1\text{-}2)$$

where 0.51 MeV is the rest mass of an electron. The probability cross-section for Compton scattering can be expressed as

$$\sigma c = \frac{CZ}{E} \qquad (1\text{-}3)$$

where C is an energy-dependent constant. Pair production occurs when a photon of at least 1.02 MeV passes very close to a nucleus; when this happens, the photon can be annihilated in the strong electrical field, with the formation of an electron-positron pair. The probability cross-section for pair production is

$$\sigma pp = TZ^2 \ (E-1.02) \qquad (1\text{-}4)$$

where T is an energy dependent constant.

In the attenuation of neutrons, the main concern is with the collisions involving nuclei. Although neutron-electron interactions do occur, the probability of such events is small. There are two possibilities involved: the neutron will bounce off and be scattered at an angle predicted by the mass of the nucleus, or the neutron will

be absorbed. The scattering may be elastic, where the conservation of energy and momentum is maintained, or inelastic, where some of the kinetic energy of the neutron is transformed into internal energy of the nucleus. Inelastic scatter may be thought of as a special case of absorption, where a delayed neutron is ejected from the nucleus. There are basically three types of absorption: capture, fission, and spallation. These latter processes are rather special and, therfore, will not be discussed. The capture process is in direct accord with the compound-nucleus theory proposed by Bohr in 1936. In his theory Bohr assumed that a nuclear reaction takes place in two steps. First the incident particle (neutron in our case) is absorbed by the target nucleus to form a compound nucleus. The compound nucleus then disintegrates by ejecting a particle (proton, neutron, alpha particle, etc.) or a γ-ray, leaving the product nucleus. However, in order for the nuclear transmutation to occur, the incident particle must have sufficient energy to penetrate the nucleus. The threshold energy for such an event is about 8 MeV, where this is the sum of the binding energy and kinetic energy of the incident particle.

Because this thesis deals directly with fast neutrons, a brief discussion of high energy neutron interactions is in order. For the low atomic number materials the majority of neutron collisions will be of the elastic-scattering type involving stationary (relative to high-energy neutrons) nuclei. The resulting shock causes the ionized nucleus to tear across the crystal lattice, snatching up electrons in its path before coming to rest in some interstitial position. The electrons dislodged by the passing nucleus will discharge their kinetic

energy by ionization and excitation of adjacent lattice atoms, until they ultimately return to the ground state or are trapped in long-lived metastable states. The effects of such collisions have yet to be explained satisfactorily; however, existing information indicates that neutron irradiation leads to decreased light output of lithium fluoride thermoluminescent dosimeters [3].

Next, consideration will be given to the interactions of resulting charged particles (beta particles, alpha particles, and protons) with nuclei and electrons. Quite obviously when the heavier particles collide with an electron the result is an inelastic shock due to the difference in masses. However, most nuclei-heavy particle interactions are generally elastic, thus creating a need for evaluating the two types of collisions separately. By evaluating the variables involved it can be synthesized that the energy loss is a function of the speed of the charged particle. In addition the loss is proportional to the atomic number of the nucleus and the square of the charge of the particle.

Although high-energy heavy particles usually undergo few deviations during their trajectory, it is important to note that they cause localized defects in solids by means of elastic collisions with nuclei. Their penetration range is usually very short, but they may cause some surface nuclei to be removed to an interstitial position. In many cases, however, much of the kinetic energy is transferred to a relatively few electrons by ionization, resulting in the formation of essentially independent fast electrons.

A collision of a beta particle with a nucleus involves a coulombic

interaction in which the electron is sharply deflected in its path. If this interaction is elastic, the process is called Rutherford scattering, and the energy of the emergent beta particle is essentially equal to that prior to the collision. Rutherford scattering is primarily responsible for backscattering of beta particles. When electrons are slowed down in the coulombic field of a nucleus, electromagnetic radiation called Bremsstrahlung is produced. This radiation is characteristic of the target nucleus and of the beta-particle energy, but is a continuum of energy and usually amounts to about 1% of the total radiation. The percentage of Bremsstrahlung production increases with the atomic number of the absorbing material. Hence, for shielding against beta radiation, it is customary to use a material of low atomic number. Bremmsstrahlung is produced by the inelastic interaction of a beta particle with the nucleus; thus, the total kinetic energy of the colliding systems is less by an amount equal to the energy radiated as Bremsstrahlung.

In beta interactions with orbital electrons the particles repel each other because of their like charges. The coulombic repulsion between a beta particle and an orbital electron may be sufficient to expel the electron completely from its atom, creating an ion pair. After this ionization process the final energy of the electron E' is less than the initial energy E by an amount equal to the sum of the binding energy E_b of the ejected electron and its kinetic energy. That is,

$$E' = E-(E_b + 1/2mv^2) \qquad (1\text{-}5)$$

Structure of Solids [4] [1]

In a gas the atoms or molecules act essentially as independent entities because of their separation distances. In a liquid, the atoms are much closer together and are held in a cohesive state by Van der Waal forces. In a solid structure the bonding forces become more pronounced and may cause the formation of regular arrangements called lattices. If the regular arrays exist the solid is said to be crystalline;[1] otherwise the solid is amorphous. Because the thermoluminescent phenomena is based on the theory of ionic crystals, the amorphous materials are ignored.

A crystal structure is a result of the minimization of energy for an ionic[2] arrangement. If a number of marbles were placed in a box, the condition of least potential energy and most stable arrangement would be a regular array where each marble plays a part in stabilizing the surrounding marbles. The crystals of most concern in this discussion are of the parallelpiped type, where each corner of the parallelpiped network, which is common to eight parallelpipeds, is occupied by an ion. A unit cell of the lattice is defined as a parallelpiped containing an ion. Because of the parallel networks, it can be seen that passing from one cell to another can be accomplished by simple translation.

---

[1] Most crystalline materials are actually polycrystalline. In a polycrystalline substance the arrangement is not strictly periodic; but there exist sub-regions called grains within the material which are periodic by are randomly oriented. The orientation changes at the grain boundary.

[2] Lithium fluoride phosphors are composed of ionic crystals.

Thus far the implications seem to be that the molecules within these lattice arrangements are bound together such that no movement occurs. In reality, however, the molecules are always slightly displaced by vibratory movements caused by thermal energy or electrostatic effects. The vibrations induced by thermal energies occur naturally, as a result of the material being at a temperature above absolute zero. The only way to reduce these is to reduce the temperature. However, it is virtually impossible to stop the vibrations caused by coulombic forces. The wave mechanics of an electron predict that the total probability of finding an electron within a prescribed region about the nucleus is equal to one. It is also possible to predict that at a particular moment an electron can be at a greater or lesser distance from the nucleus than is required for ionic equilibrium. Thus, for this particular moment the coulombic forces will cause the nucleus to move toward or away from the electron depending upon its location. Because electrons have movement even at absolute zero this electrostatic effect can never cease to exist. This energy is associated with entropy and is termed in thermodynamics to be non-available.

Quantum mechanics predicts that these vibratory energies can only vary by certain quanta called phonons (all phonons do not have the same energy). It can be shown that the energy of a phonon is given by the expression

$$E = h\nu_c \qquad (1\text{-}6)$$

where ν_c is one of the classical resonant frequencies of an elastically tied atomic system, and h is Planck's constant. A phonon may be

considered to be a superposition of two waves of wavelength λ spreading in a certain direction with opposite speeds. It may be termed a sort of non-relativistic photon where its wavelength is related to the speed of the elastic wave, u, and ν_c by:

$$\lambda = u/\nu_c \; ; \qquad (1\text{-}7)$$

thus, the momentum of the phonon is

$$P = \frac{h\nu_c}{u} = \frac{E}{u} \qquad (1\text{-}8)$$

Therefore for the same energy, a phonon has greater momentum than a photon because u is much less than the speed of light.

The initial explanation of electron theory starts with the hypothesis that the atoms are stationary and are arranged in a three-dimensional periodic field in space. The electrons are assumed to be of two types; those closest to the nucleus that are only slightly influenced by surrounding atoms, and those loosely bound to the nucleus which become part of the valence band, characteristic of the lattice, by virtue of their overlapping orbitals. Quantum mechanics predicts that these electrons will exist in certain quantized energy bands, between which may exist energy gaps. The value of the energy of an electron, however, does not entirely describe the state of that electron. It becomes necessary to introduce the wave mechanics of electrons and the resulting wave function ψ which takes into account other variables in addition to energy. As it turns out, if the crystal contains N elementary cells, the number of discrete wave functions is

N. As there are always two possible values of spin, each allowed a band corresponds to 2N characteristic states which is equal to the number of electrons a band may contain. Thus, although the energies are of a quantized nature, they form a quasi-continuous band, which for most purposes can be considered a continuum of energies.

The solutions for the wave-equation define the energy ranges for the bands; however, a thermodynamic evaluation is necessary to associate the electrons with a particular band.

$$G = U - TS + PV \qquad (1\text{-}9)$$

where: U = internal energy; S = entrophy; V = volume; T = absolute temperature; P = pressure. If the assumptions are made that (1) there is no exchange of electrons between bands (the volume and pressure remain constant) and (2) the temperature is taken to be absolute zero, then the internal energy must be made to be a minimum. For this condition the electrons fill the lowest energy bands, such that there are no electrons with energy greater than a maximum energy, E_f. If the number of electrons is odd, then the last band contains N electrons. Thus there remain N vacant states in this band. If the number is even, then a division by two dictates the number of bands exactly filled, at least inasmuch as the last filled band has no common part with the following band of greater energy. For an insulator, this last filled band is called a valence band; and the one immediately higher, which is normally empty at absolute zero, is called the conduction band. As was mentioned earlier the region between is the forbidden gap for ionic crystals. For a metal, however, the valence and conduction bands share

a common part. They accept electrons up to the level E_f, but neither is filled.

Figure 1-1. Energy Band Arrangements

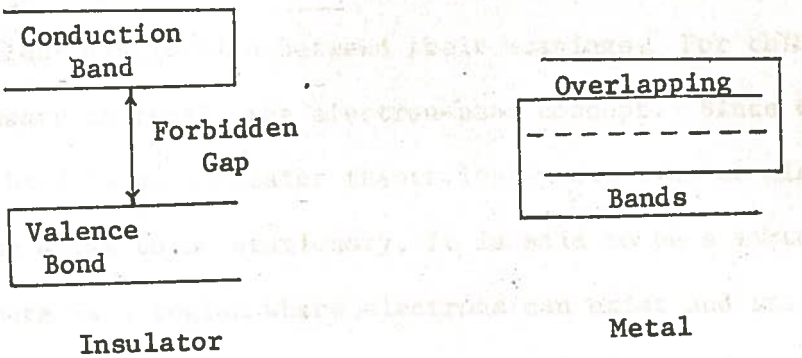

Insulator Metal

In relation to the above discussion, a note in regard to electrical conductivity would be in order. If a band is entirely filled, the flow of electrons is impossible according to quantum mechanics. Thus it becomes obvious that a conductor must be a material whose valence and conduction bands overlap, and neither band is filled. Accordingly, an insulator has the valence and conduction bands separated by the forbidden gap. However, it should be noted that an unfilled valence band contributes to conductivity.

The principle of indiscernibility or exclusion of Pauli shows that once the temperature increases to some value above absolute zero, some electrons are to be found in states that were vacant originally, and less electrons are to be found in the filled band. This phenomena can be explained by considering the phonon again. As the temperature increases, more thermal vibrations of the atoms are observed, causing an increase in phonon population. These phonons then collide with electrons, imparting all or part of their energy to the electrons.

The electrons are then passed to a state of higher energy in a vacant band. It is also possible for an electron to fall to a state of lower energy and in the process emit a phonon or photon or both, simultaneously.

The terms ionization and excitation have been used previously without a clear distinction between their meanings. For this discussion it is necessary to recall the electron-band concept. Since the conduction band in an insulator theoretically contains no electrons, assuming the atoms to be stationary, it is said to be a virtual band. That is, there is a region where electrons can exist and still be considered as part of the lattice structure if they achieve sufficient energy to be extracted from the valence band. Thus excitation is the process whereby an electron gains the necessary energy (from photon collisions or whatever) to become part of a virtual energy band. There is an energy, however, at which any additional collisions will cause the electron to leave the lattice arrangement and become a free electron. This energy is called the ionization energy, E_i, and this process is called ionization. After the electron attains this free state, the laws of quantum mechanics predict that the electron can assume any energy above E_i. Thus, above the quantized states, there exist a continuum of states for which there is no quantization of the energy. The energy band with E_i as the upper limit is termed the last band of the fundamental state.

In conjunction with the discussion of excitation of electrons, it becomes necessary to introduce the existance of an unusual type of defect called an exciton. An exciton occurs when by some means an electron reaches the conduction band of an insulator, and then associates

itself with a vacated hole in the valence band. This combination acts as sort of a hydrogen atom for which the energies of the excited states lie somewhere in the forbidden zone. By virtue of the neutrality created by this association, the exciton is free to migrate within the forbidden gap. The ground state of an exciton corresponds to the electron and hole in the originating valence band; the ionization potential corresponds to the lowest energy of the conduction band. Excitons are mentioned only because later it will be shown how they effect thermoluminescence.

Figure 1-2. Sketch of the Electronic Levels of a Perfect Insulator.

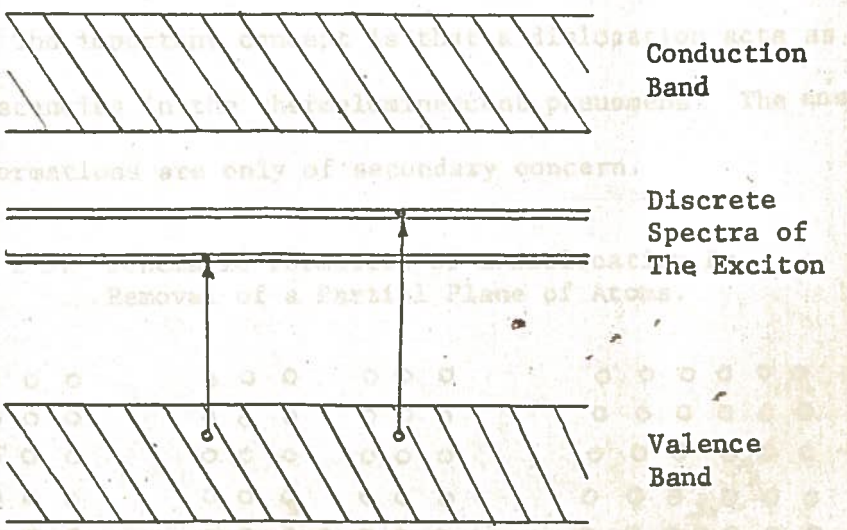

Lattice Defects in Ionic Crystals [4] [1]

The question as to how to classify defects in solids is not strictly resolved; however, in general, anything which causes the lattice to deviate from perfect periodicity is considered to be a defect. The subdivisions seem to be dislocations, Schottky and Frenkel defects and their derivates, and impurities.

Most of the information concerning dislocations was discovered while trying to explain the slip process in metallurgy. The calculations of the necessary stress to cause slipping of parallel planes of crystals did not coincide to experimental values. Through the efforts of Taylor, Orowan, and Polanyi, the concept of dislocations was developed to explain this deviation, although their origins are still unexplained. A dislocation is essentially a series of point vacancies which constitue a continuous plane. With the two-dimensional schematic below it is possible to visualize the lattice rearrangement as a result of such a vacancy. The important concept is that a dislocation acts as a series of vacancies in the thermoluminescent phenomena. The ensuing plastic deformations are only of secondary concern.

Figure 1-3. Schematic Formation of a Dislocation By Removal of a Partial Plane of Atoms.

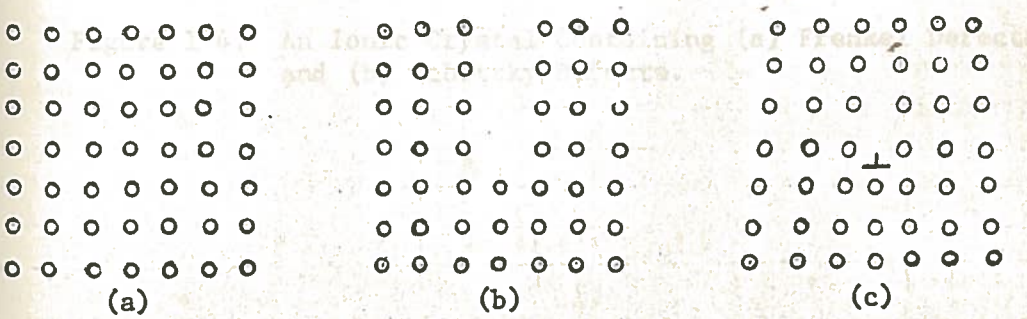

To explain Schottky and Frenkel defects it is necessary to recall the periodic lattice arrangement discussed initially. Instead of calling every point in the lattice at atom, however, the ionic crystal is introduced. In these alkali-halide arrangements the valence electron of the metal atom spends more time in the vicinity of the halogen. Thus the halogen, in a sense, becomes an anion as a result of the newly acquired electron, and the alkali is a cation; the periodicity in space is still maintained however. These localized charges can then give rise to defects. One such defect is called a Frenkel defect and is just a cation or anion vacancy-interstitial pair. A vacancy is the absence of an ion at a point in the lattice, and an interstitial is the presence of an ion at some location other than a point in the lattice. If a cation vacancy and an anion vacancy occur together, the defect is called a Schottky defect.

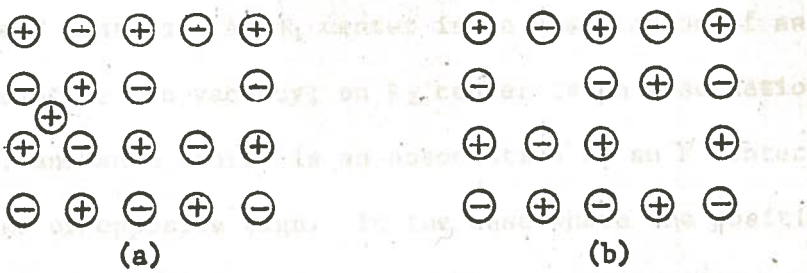

Figure 1-4. An Ionic Crystal Containing (a) Frenkel Defects, and (b) Schottky Defects.

It should be pointed out that the net result of such defects is neutrality; therefore, no counteracting charge is necessary for stability.

From these concepts it is evident that a negative ion vacancy creates a localized coulombic field analogous to a positive charge, and vice versa. This field then attracts electrons in the conduction band that are close enough to be influenced and causes them to gravitate in orbits (wave functions) around the vacancy. When such an electron becomes trapped this is called an F center or color center. The F centers are also characterized by quantum energies and thus constitute an F band. If incident photon wave lengths fall within the F band, the absorption decreases in this region, and there appears a new absorption band of F' centers, where F' centers are negative ion vacancies which have two trapped electrons.

There may also exist R_1, R_2, and M centers which serves in conjunction with the F centers. An R_1 center is an association of an F center and a negative ion vacancy; an R_2 center is an association of two F centers; and an M center is an association of an F center with two vacancies of opposite sign. In the case where the positive ion is trapped by a positive ion vacancy, the exact opposite to the F center, there are created V_1 centers. These in turn lead to V_2 centers (association of two V_1 centers), V_3 centers (association of a V_1 center and a positive ion vacancy), and V_4 centers (association of a V_1 center with two vacancies of opposite signs).

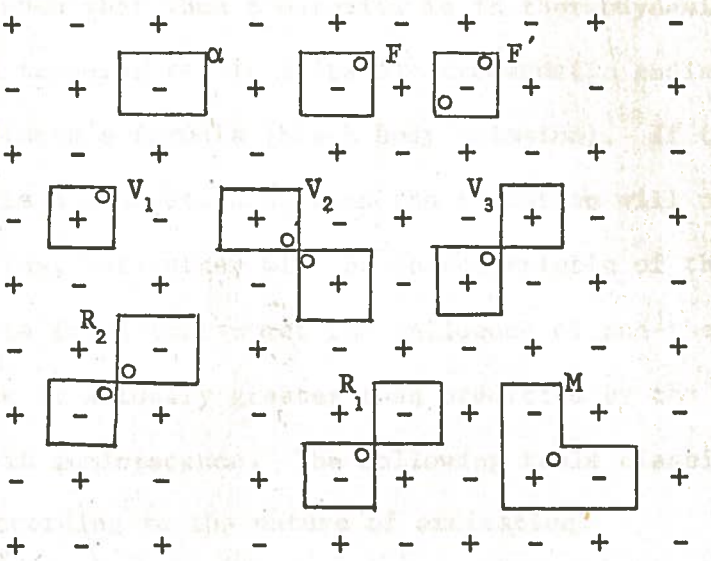

Figure 1- 5. Model of Several Types of Color Centers in Alkali Halide Crystals

In addition to defects that exist within pure materials, there are also cases where foreign substances disturb the lattice arrangment. These are called impurities and may constitute a good percentage of lattice disorder. The term impurity is designated as an atom of a substance normally absent in a pure crystal, and does not refer to non-uniformity within the crystal. Impurities may exist in regular lattice positions or as interstitials. Because their quantized energies are different they cause local perturbation of normal lattice wave functions and as a result may serve as a foundation for electron traps.

Fundamental Mechanisms of Thermoluminescence [4]

It is known that when a material is in thermodynamic equilibrium at a certain temperature, it emits electromagnetic radiation in accordance with Planck's formula (black body emission). If thermodynamic equilibrium is not maintained, then the radiation will not conform to Planck's Law, but rather will be characteristic of the substance. However, it is found that under the influence of non-thermal excitation, the luminance is actually greater than predicted by the black body model; this is luminescence. The following table classifies luminescence phenomena according to the nature of excitation:

Excitation Nature	Phenomenon Name
Any particles at relativistic speeds in refringent media	Cerenkov effect
γ, X-rays	Roentgenoluminescence
α particles, ions	Radioluminescence
Electrons or rays	Cathodoluminescence
Low energy photons (a few eV)	Photoluminescence
Mechanical actions (fracture for example)	Triboluminescence
Alternating electric field	Electroluminescence
Chemical reactions energy	Chemicoluminescence
Biochemical reactions energy	Bioluminescence

The fundamental concept of light emission is that the visible region of electronmagnetic radiation is about 2 or 3 ev, which corresponds to the width of the forbidden band of an ionic crystal. This means that if the ground state of an electron is within the valence band, then the electron must be trapped in the forbidden gap for visible light to be given off. The only possibility of a pure transition occurs at the extreme boundaries of the conduction and valence bands; however, there is no storage mechanism, thus thermoluminescence is impossible. From published literature the determination of the type of trap causing thermoluminescence is a matter of speculation. Besides thermoluminescence an electron may become trapped such that it (1) cannot be released without excessive thermal excitation, (2) de-excites at room temperature, or (3) de-excites by a mechanism which does not involve the emission of electromagnetic radiation. Therefore, to discuss the thermoluminescent phenomena it is necessary to propose a basic formulation of the kinetics to explain the Gaussian-shaped glow curves.[3] Recalling that most of the energy of incident radiation reduces to excitation of electrons, a proposal would necessarily involve their ultimate fate. Because neutrons primarily excite electrons through secondary interactions, gamma radiation appears to be a more attractive subject in such an endeavor. Certainly, however, a similar proposal could be made for neutrons with slight modifications.

By assuming that (1) excited electrons migrate through the conduction band or associate with holes creating excitons, and (2) the electrons may become trapped in metastable traps which de-excite upon

---

[3]See Appendix I.

addition of heat by a radiative or non-radiative emission, it is possible to express the glow curves as a sum of two exponentials.

$$\frac{d[e_T]}{dt} = \left(A_r e^{-E_r^*/R\sqrt{at+b}} + A_{nr} e^{-E_{nr}^*/R\sqrt{at+b}}\right)[e_r] \quad (1\text{-}11)$$

where $\frac{d[e_T]}{dt}$ is the rate of de-excitation of electrons from metastable traps, (2) t is the time associated with addition of heat, (3) R is the gas constant, (4) A_r, A_{rn}, E_r^*, E_{nr}^*, a, and b are system constants, and (5) $[e_r]$ is the concentration of trapped electrons. Such an expression predicts that the dormant regions in the thermoluminescence spectra are due to the non-radiative traps.

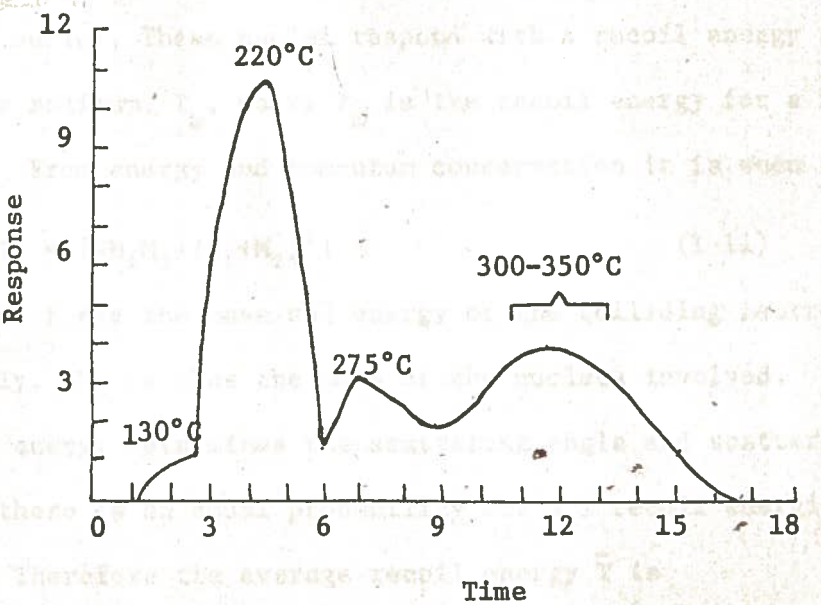

Figure 1-6. LiF Characteristic Glow Curve.

Radiation Damage [9] [10]

The term damage can be misleading in some cases because the induced changes may be either harmful or beneficial. A more descriptive term may be radiation effects by gamma and neutron bombardment. For simplification the treatment of each case will be made separately.

As was discussed earlier, the traps causing thermoluminescence are a result of defects in the crystal structure. These defects can be loosely catagorized as vacancies, interstitials, and impurities. The introduction of impurities other than those naturally occuring is by nuclear transmutations; therefore, the major concern of high energy radiation damage is that of the vacancies and interstitials created. Since neutrons, as their name implies, are neutral in charge the only type of interaction which can occur is of a direct collision nature involving, principly, nuclei. These nuclei respond with a recoil energy varying from 0 to a maximum, T_m, where T_m is the recoil energy for a head on collision. From energy and momentum conservation it is seen that

$$T_m = [4M_1M_2/(M_1+M_2)^2]\ E \qquad (1\text{-}11)$$

where M_1 and E are the mass and energy of the colliding neutron, respectively. M_2 is thus the mass of the nucleus involved. Since the recoil energy determines the scattering angle and scattering is isotropic there is an equal probability for all recoil energies between 0 and T_m. Therefore the average recoil energy $\overline{T}$ is

$$\overline{T} = 1/2\ T_m \qquad (1\text{-}12)$$

Thus for 14 MeV neutrons the mean recoil energy for Li is 4 MeV and F

is 1.47 MeV. This is not to imply that more energy is transferred to low Z materials, because consideration must be given to the probability of interaction. A good measure of a materials ability to absorb neutron energy would be the product of $\overline{T}$ and the elastic scattering probability.

If a nucleus receives greater recoil energy than a certain minimum energy required for dislocation, E_d, it leaves its stable position in the lattice and is termed a displacement. The number of these primary displacements per unit volume produced by neutron bombardment can be expressed by

$$n_p = \phi t n_o \sigma d \qquad (1\text{-}13)$$

where ϕ is the neutron flux (neutrons/cm^2-sec), t is the irradiation time (sec), n_o is the number of target atoms per unit volume, and d is the cross-section per atom for producing displacements.

If the recoil energy of the nucleus is sufficiently greater than E_d, then other displacements may be produced from collisions with other nuclei. Thus, by definition, $\overline{\nu}$ is the average number of displaced nuclei per neutron collision, such that

$$N_d = n_p \overline{\nu} \qquad (1\text{-}14)$$

where N_d is the total number of displaced atomcs per unit volume. The calculation of $\overline{\nu}$ for a particular medium and neutron energy, however, becomes a very complex task because of the possibility that the second collided nucleus will also cause additional displacements. This effect could continue and multiply in accordance with a geometrical progression, such that, $\overline{\nu}$ would become a complex function.

For an analysis of $\overline{\nu}$ it becomes necessary to consider the possible fate of a displacement. Because of the energies involved, the collided nucleus will recoil with a velocity large enough to leave behind valence electrons and will act as a charged particle. As with any charged particle the excess energy must be absorbed by ionization with electrons or by direct collisions with other nuclei. For this analysis the following assumptions are made:

(a) The collided nucleus loses energy entirely by ionization until its kinetic energy falls below the limiting energy for ionization, E_i.

(b) All collided nuclei with energy below E_i lose energy only by elastic collisions with lattic atoms.

(c) An atom will be displaced from its lattice site if by collision it receives kinetic energy greater than E_d, and will never be displaced if it received less than E_d.

With this model the calculation of $\nu(E)$ becomes a matter of evaluating the possible fates of recoil nuclei for any particular energy. By integrating this function times a probability function over all possible energies a general expression for $\overline{\nu}$ is obtained. The value of $\overline{\nu}$ for charged particles can be calculated from the equation

$$\overline{\nu} = 1/2 \frac{T_m}{T_m - E_d} \left(1 + \ln \frac{T_m}{E_d}\right) \qquad (1\text{-}15)$$

This is adaptable for this case by the assumptions of a single collision occuring per neutron, and the resulting collided nuclei acting as a charged particle.

The other obvious possibility which was neglected above is that of replacement collisons. These occur when the striking atom remains behind at the collision site. The struck atom then receives energy greater than E_d and the incoming atom is left with energy less than E_d. The development of the number of replacements per primary collisions is very similar to that of displacements. The model is directly adaptable from the above with slight modifications to allow for the cohesive bonding of lattice atoms. The replacement theory also allows for the possibility of both atoms remaining at one lattice position if neither has kinetic energy greater than some minimum energy E_r, after the collision.[4] Obviously the value of E_r must be smaller than E_d and varies with each material. A material-dependent function, $\mu(E)$, is then the average number of replacements generated by a moving atom of energy E and is developed similarly to $\nu(E)$.

The end product for fast neutron bombardment is

$$\frac{\text{number of atoms replaced}}{\text{number of atoms displaced}} = 1.614 \ln \frac{E_d}{E_r} + 1 \qquad (1\text{-}16)$$

This ratio thus predicts that in the case of fast neutrons there are about five replacements per displacement. In the final analysis, however, these calculations are not accurate because atoms are affected in groups. Instead of the simple single atom replacement-displacement theory, it is necessary to consider displaced regions called spikes. Thus the foregoing calculation of five replacements per displacement is

[4] Unfortunately no direct calculations of E_r have been made, but experimental evidence suggests that $E_{d/E_r} = 10$.

not an accurate computation, but must be regarded only as an estimate of the general nature of the effects of fast neutrons. The main source of impurities other than those that exist naturally in the virgin crystal is neutron transmutation. For this, consideration will be mainly focused on 14 MeV neutrons, which are a result of the $^{3}H(d,n)$ He reaction, and 2.44 MeV neutrons, which are a result of the $^{2}H(d,n)^{3}He$ reaction. Below is a chart of possible interactions and their probability of occurance. Of natural Li only ^{6}Li is listed because ^{7}Li is virtually insensitive to neutrons. In these reactions, it should be noted that the induced radiation may play a significant part in neutron damage (i.e., the localized damage due to the (n,α) reactions).

Reaction	σ (barns)		Half-Life	Daughter
	14 MeV	2.44 MeV		
$^{6}Li(n,p)^{6}He$	.0064	.01	.82 sec.	^{6}Li
$^{6}Li(n,\alpha)^{3}H$	.025	.20	12.46 yrs.	^{3}He
$^{19}F(n,p)^{19}O$	.140	below threshold	29.4 sec.	^{19}F
$^{19}F(n,2n)^{18}F$	.06	below threshold	112 min.	^{18}O
$^{19}F(n,\alpha)^{16}N$	.140		7.36 sec.	^{16}O

The decay radiation for most of these reactions also produce a certain amount of excited electrons. They are mainly very energetic betas ranging from a 10.4 MeV electron from ^{16}N to a 17.6 KeV electron from ^{3}H. In addition, there is a 7 MeV gamma emitted from ^{16}N; however, its long mean free path virtually assures its escape from the LiF powder before interacting.

To gain some insight as to the degree of impurities created, the activity can be calculated for the particular transmutation form the formula:

$$A = Nk\sigma\phi S \qquad (1\text{-}17)$$

where, (1) A = activity (disintegration/second-gram)

(2) N = number of atoms of original element per gram

(3) k = fractional abundance of isotope present in the element

(4) σ = activation cross-section of isotope (cm^2)

(5) ϕ = neutron flux ($n/cm^2/sec$)

(6) S = saturation factor = $1-\exp[-.693t/T_{1/2}]$

(7) t = irradiation time (seconds)

(8) $T_{1/2}$ = half-life of activated species (seconds)

Ionization is the most important mechanism in gamma radiation. It causes the production of high-energy electrons which may (1) collide with nuclei to produce relativistic Rutherford scattering and possibly displacement production, or (2) interact with valence electrons to produce color centers. For the first case the probability is small because of the energies involved; however, the second case has a definite effect on the thermoluminescent properties of a crystal.[5] One such effect involves the movement of the created excitons through the forbidden zone and the discharge of their energy into the lattice upon encountering irregularities. This produces a local hot spot and possibly a dislocation climb. The energies available are on the order

[5] According to Ehrlich [11] there is a good possibility that F centers do not contribute to thermoluminescence because of their dose rate independence.

of 10 ev, which is sufficient to create a vacancy. A second effect, which applies mainly to ionic crystals is the production of F centers and its derivates. This occurs when a high speed electron strips the negative charge from an anion and forces the neutral atom into an interstitial position. The positively charge vacancy created then attracts an electron to form an F center or a derivate. According to Varley [12] F centers are formed during gamma irradiations in large quantities.

The last process of concern in radiation effects is that of annealing. Essentially, the defects produced by irradiation are capable of moving about if the temperature is sufficiently high. In this way the damage is altered, and, possibly, eventually annealed out. The first approximation would be, therefore, that the altering of damage for ionic crystals would be proportional to the mobility of the defects. From electrical conductivity experiment it has been confirmed that defect mobility equals a constant time $(T^{-1})[\exp(-E_m/kT)]$, where E_m is the activation energy (E_m = .65 ev for LiF).

The process of annealing point defects involves their diffusion in the lattice until they are immobilized by traps or are absorbed by sinks. Vacancies and interstitials can combine or annihilate each other, or they can be absorbed in irregularities. Impurity interstitials may combine with vacancies to form substitutions such as jogs in dislocations, and substitutional impurities may then induce local stress fields and trap vacancies and interstitials, or conversely be replaced by larger interstitials. These mechanisms, in a sense, summarize what can and usually does happen during an annealing operations. The actual mathematical treatment of annealing effects is beyond the scope of this thesis.

Literature Review

Although there is much work being performed at present, the current available published literature on radiation damage in thermoluminescent dosimeters is rather sketchy. The first article of interest in this field was published by Marrone and Attix [1] in early 1964. Their approach consisted of first verifying the established photomultiplier current (thermoluminescence) versus exposure curve for LiF. The curve (Figure 1-7) is linear to $\simeq 10^3$R, where it becomes superlinear with the response being proportional to the 1.2 power of the exposure. This continues until saturation of the lower traps occurs and a maximum dose is reached.[6]

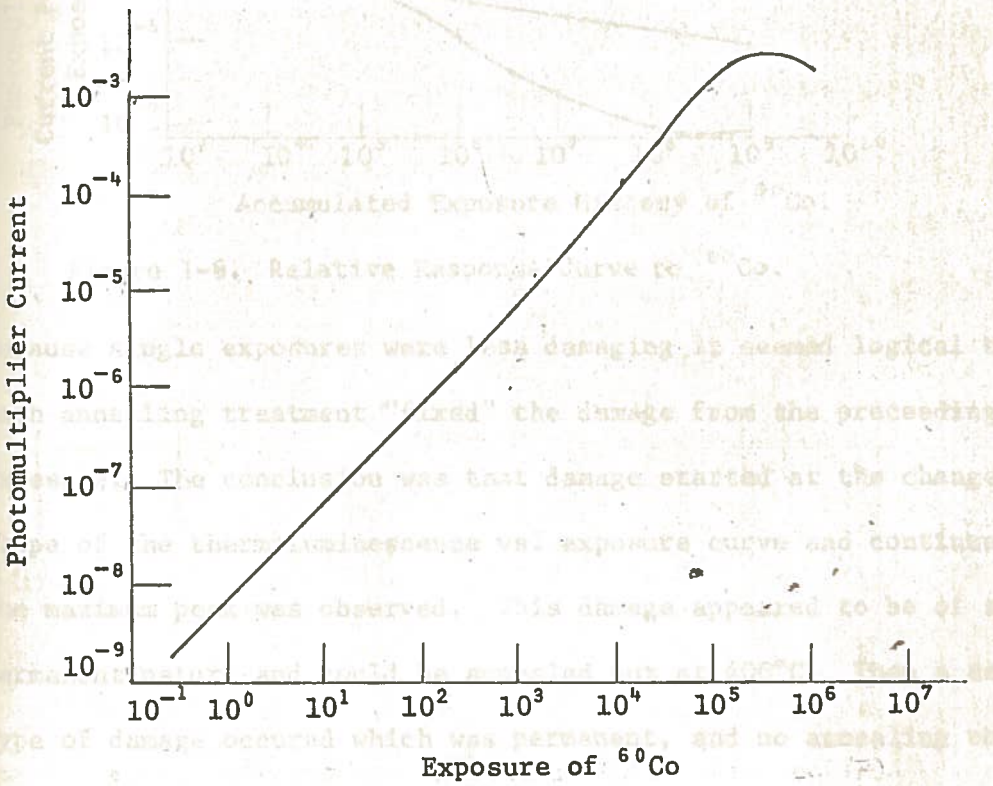

Figure 1-7. Thermoluminescent Response of LiF.

[6] Two years later R. M. Hall [13] observed that this maximum dose could be extended by evaluating the second glow peak.

Linearity loss seemed to suggest a possible damage mechanism which could be of a permanent nature to the thermoluminescent response. Thus by utilizing a uniform ^{60}Co dose a relative response was calculated, and it was found to decrease drastically at high doses for LiF (Figure 1-8). The main concern was whether this was radiation damage, annealing damage, or both since the points did not represent a single exposure. By repeating the experiment for only single exposures the second line was obtained.

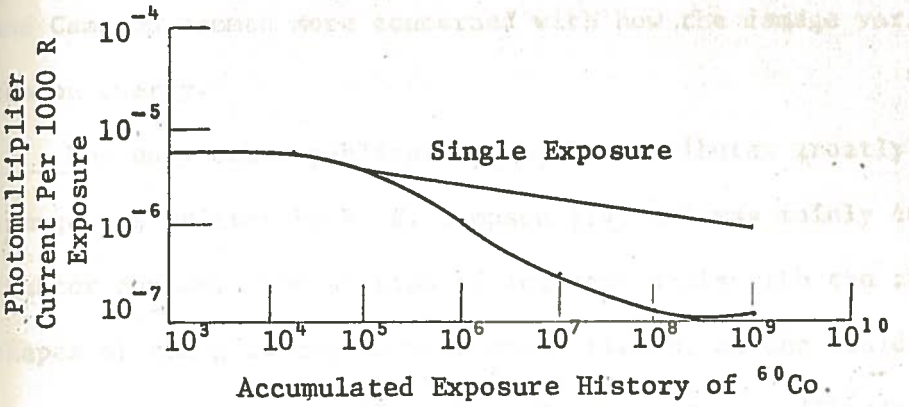

Figure 1-8. Relative Response Curve to ^{60}Co.

Because single exposures were less damaging it seemed logical that each annealing treatment "fixed" the damage from the preceeding exposure. The conclusion was that damage started at the change in slope of the thermoluminescence vs. exposure curve and continued until the maximum peak was observed. This damage appeared to be of the non-permanent nature and could be annealed out at 400°C. Then a second type of damage occured which was permanent, and no annealing short of melting the phosphor could remove it. This appears to occur at the maximum response peak.

The next research of importance by Doppke and Cameron [2] was very similar in nature to Marrone and Attix work. The main difference, however, was that a mathematical formulation was made for the change in sensitivity. It seemed that the damage could be accurately described by the sum of two exponential functions, where the first exponential was due to damage of unfilled traps and the second was due to damage of filled traps. Their maximum exposure was only 2.5×10^6 R, therefore, applying this generally would be presumptuous. In addition Doppke and Cameron seemed more concerned with how the damage varied with photon energy.

The only other publication which contributes greatly to photon damage was written by R. E. Simpson [14] and was mainly concerned with reactor gammas. The section of interest deals with the change in the shapes of the glow curves with mixed fields, as one would expect in a reactor, when compared to the pure gamma curves (Figure 1-9). This suggested that neutrons cause thermoluminescence by a different mode than gammas; thus, neutron damage may be quite different from gamma damage.

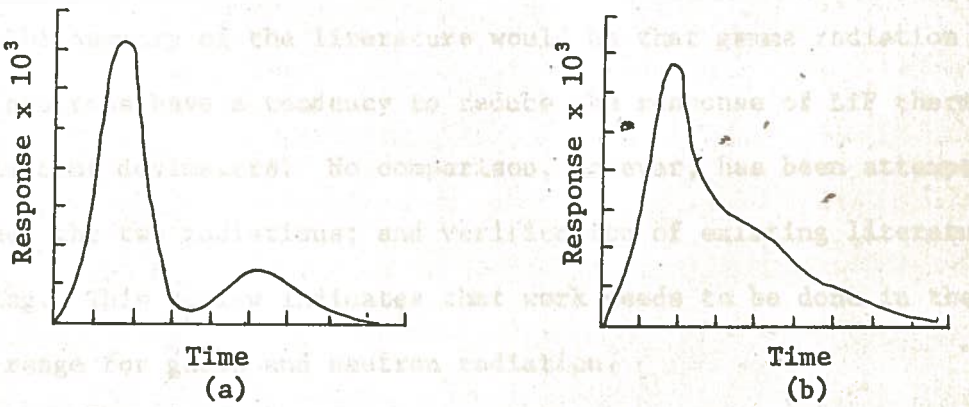

Figure 1-9. LiF Glow Curves for a (a) ^{60}Co Exposure, and (b) Reactor Exposure.

In early 1966 Kastner, Oltman, and Tedeschi [15] published the results of their work on fast neutron response. By utilizing reactor neutrons and the 4.5 MeV neutrons from a Van de Graff, their approach was to determine thermoluminescent response as a function of the neutron energies. The ever existing $^{6}Li(n,\alpha)^{3}H$ reaction, which has a thermal cross-section of about 950 barns, however, seemed to plague their results.

They continued their research with fast neutrons and about one year later published work concerning the effects of fast neutrons on TL response of gamma rays [3]. This was actually the first literature available which dealt specifically with neutron damage. The paper appeared to be slanted toward possible applications for using TLD in reactors for purposes of measuring gamma radiation. The procedure was to expose the dosimeters to a uniform dose of ^{60}Co gamma and then to a fast neutron dose varying from 0.1 to 1 MeV. These were then read and compared to dosimeters only experiencing gamma exposures. The fast neutron exposure consistently reduced the readout by 10%, appearing to be a damage mechanism.

The summary of the literature would be that gamma radiation and fast neutrons have a tendency to reduce the response of LiF thermoluminescent dosimeters. No comparison, however, has been attempted between the two radiations; and verification of existing literature is lacking. This review indicates that work needs to be done in the high dose range for gamma and neutron radiation.

EXPERIMENTAL TECHNIQUES

Equipment

The foremost consideration as to equipment must obviously be given to the lithium fluoride thermoluminescent dosimeters and TLD reader. The reader is model number E-1V manufactured by Madison Research Inc. and the dosimeters are TLD-100 manufactured also by MRI. The reader utilizes a pure silver planchet to contain the dosimeters, and varying current through the planchet serves as a heating mechanism. The readout is a visual type and integrates the area under the glow curve, rather than giving a peak height. This integration produces a pure number from which calibration curves must be drawn for dose measurements. The heating cycle is thirty seconds in length and temperature control is maintained by a dial ranging in numbers from 1 to 100. For low doses the photomultiplier tube voltage can be adjusted for greater sensitivity, and a nitrogen quench is used throughout the cycle to reduce tribo thermoluminescence. In most of the experiments TLD-100 powder is used because of its high melting point. Annealing procedures in the 650°C range cannot be tolerated by the extruded TLD rods incapsulated in a teflon matrix. For comparison purposes, however, one of the experiments utilize some of these TLD-100 rods. The designation of TLD-100 is simply a terminology for the natural lithium which contains 92% ^{7}Li and 8% ^{6}Li. Other types include TLD-600, which is highly enriched in ^{6}Li, and TLD-700, which is almost pure ^{7}Li. The latter would be used because of its insensitivity to neutrons. The TLD powder is measured by means of a powder dispenser, another product of

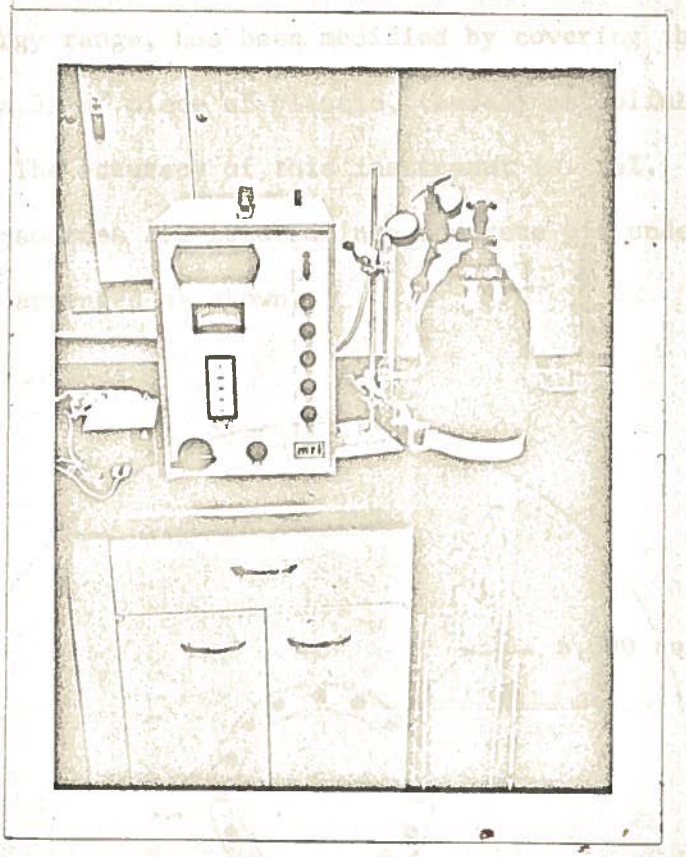

Figure 2-1. Dosimeter Reader System

of MRI, which transfers 35 mg. with an accuracy of ±2%. The dispenser utilizes a vibrator to insure uniform packing of the powder.

The gamma exposures are obtained from two ^{60}Co sources. One, a 30,000-Ci source, has a dose rate of about 1.15×10^4 R/min; and the other a 6,000-Ci source, has a dose rate of 1.00×10^3 R/min. These dose rates are obtained from a Radocon, model 575, manufactured by Victoreen, using a model 602 probe. The probe, which was for a different energy range, has been modified by covering the detection chamber with a 3/16" piece of plastic, thereby establishing electronic equilibrium. The accuracy of this instrument is ±5%.

The ^{60}Co-sources are located in a concrete pit under 16 feet of water and are arranged as shown.

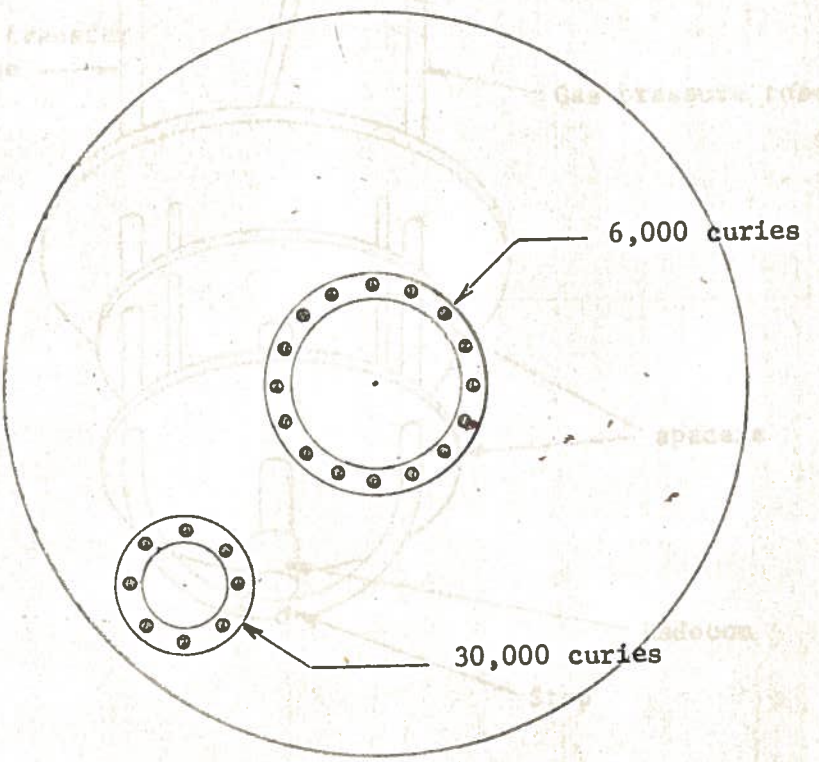

Figure 2-2. Cobalt-60 Irradiation Pit. Plan View.

The most practical way of using the 6,000-Ci source is by means of a diving chamber. By modifying the top to the diving chamber as shown below, the dose rate is known and rapid transfer of the dosimeters is possible. A similar arrangement for the large source is also used with the exception that a detection probe is not part of the device. A cross reference using the TLD powder is used to calibrate the large source. Pressurized nitrogen is used to "blow" the dosimeters in and out of the diving chambers.

Figure 2-3. Rapid Transfer Arrangement.

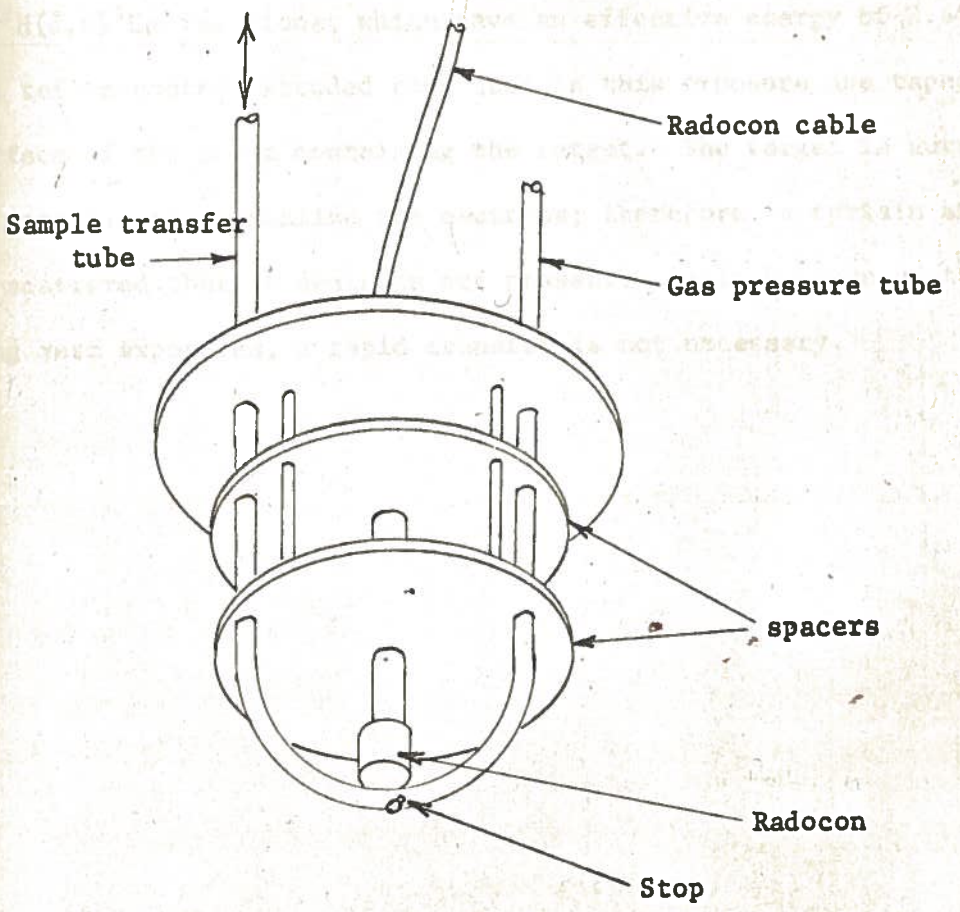

The fast neutrons are obtained from a Cockroft-Walton accelerator manufactured by Texas Nuclear Corp. From the $^{3}H(d,n)^{4}He$ reaction are produced essentially monoenergetic neutrons of 14 MeV energy which serve as a basis for the neutron experiments. The TLD-100 powder is arranged around the peripheral of the target in such a manner as to eliminate, as much as possible, induced gamma radiation and scattered neutrons. The long term exposures eliminate the need for a rapid transfer mechanism.

The remaining neutron exposures were obtained through the facilities of Accelerators, Inc. of Austin, Texas. The neutrons are the result of $^{2}H(d,n)^{3}He$ reactions, which have an effective energy of 2.44 MeV. The teflon-coated extruded rods used in this exposure are taped to the surface of the snout containing the target. The target is surrounded by paraffin to thermalize the neutrons; therefore, a certain amount of scattered thermal neutrons are present. Again because of the long term exposures, a rapid transfer is not necessary.

Procedures

The procedures involved with the care of the lithium fluoride powder are in agreement with accepted standards as set forth by Cameron, et al. [16]. When the powder was received it was annealed at 400°C for one hour and then rapidly quenched to room temperature to release any trapped electrons. Following this the powder was annealed at 80°C for 24 hours to reduce the amount of low temperature traps. The powder was then exposed and just before reading another annealing process at 100°C for 10 minutes was done to eliminate all but the main glow peak. The photomultiplier tube voltage was set at 1000 volts for most of the readings, and the low-gain setting was employed. The temperature selection was set at 47.5, which produced a maximum planchet temperature of 245°C. Efficiency curves were run for the amount of TLD powder versus thermoluminescence for a given dose, and it was found that 35 mg. samples were best.

In the gamma radiation damage section the TLD-100 powder was used exclusively. By use of the rapid transfer mechanisms described earlier the dosimeters were exposed to damaging doses ranging from 10^3 to 10^8 R. To verify the PMT current versus dose curve as reported by Cameron [16] the dosimeters were then read at 800 volts. The standard procedure for annealing was repeated, and the damaged dosimeters were exposed to a uniform dose of 1000 R. The dosimeters were read again, this time at 1000 volts, to ascertain any induced damage. To determine if annealing caused the restoration of response, a second annealing was done at 500°C for one hour followed by a uniform dose. The differences in TL were again recorded. Lastly, an annealing at 600°C was performed

and the cycle repeated.

This general procedure for the powder was repeated twice more, each yielding similar damage phenomena. By maintaining a control subjected to no damage dose but all annealing procedures, a relative response of the damaged dosimeters could be obtained from the term S_D/S_v; where S_D is the TL of the damaged dosimeter, and S_v is the TL of the virgin crystal. To produce a more descriptive graph the relative response could be represented as $(1-S_D/S_v)$ and plotted versus dose. It soon became apparent that by plotting a logarithmic value of dose the data gave the appearance of being linear, indicating the presence of a first order kinetics relationship. By using the method of least squares[7] a best fit equation was obtained for all three annealing temperatures of the form:

$$(1-S_D/S_v) = m \ln D + b \qquad (2\text{-}1)$$

To determine how low temperature annealings fix the damage [1] a series of virgin dosimeters were exposed to varying damage doses to 4×10^6 R and then annealed at 600°C for one hour.

For the 14 MeV neutron irradiations the powder was placed in a plastic bag and rolled up to form essentially a line geometry. This was then taped around the peripheral of the target of the Cockcroft-Walton accelerator and irradiated for various times. The dosimeters were then annealed according to the standard procedure and exposed to gamma radiation. There were two groups of neutron exposures, and each group was divided into five sub-groups. Each sub-group was

---

[7] See Appendix III

exposed to a different gamma dose ranging from 1×10^3 to 7×10^3 R with controls being maintained. The dosimeters were then read according to the standard regime, and the relative responses compared.

The last section dealt with fast neutron irradiations of extruded LiF rods incapsulated in a teflon matrix. The rods were taped to the target and irradiated for various times. They were then annealed at 250°C for one hour followed by a 24 hour annealing at 80°C. There were three groups of rods and each was exposed to 1000 R.

RESULTS

The experimental data of $(1-S_D/S_v)$, which are located in Appendix II, were plotted as a function of the logarithm of the dose for 400°C (Figure 3-1), 500°C (Figure 3-2), and 600°C (Figure 3-3) annealings. By the method of least squares[8] the following best fit equations were obtained:

1) 400°C annealing

$$(1-S_D/S_v) = 0.0680 \ln(D) - 0.499 \qquad (3-1)$$

2) 500°C annealing

$$(1-S_D/S_v) = 0.0460 \ln(D) - 0.371 \qquad (3-2)$$

3) 600°C annealing

$$(1-S_D/S_v) = 0.0152 \ln(D) - 0.0819 \qquad (3-3)$$

The annealing of the damaged dosimeters at 600°C without any previous annealings apparently completely restored the response for doses to 4×10^6 R.

The damage to the LiF from the fast neutrons was found to be negligible. The change in response was so small no conclusive statements could be made.

---

[8] See Appendix III.

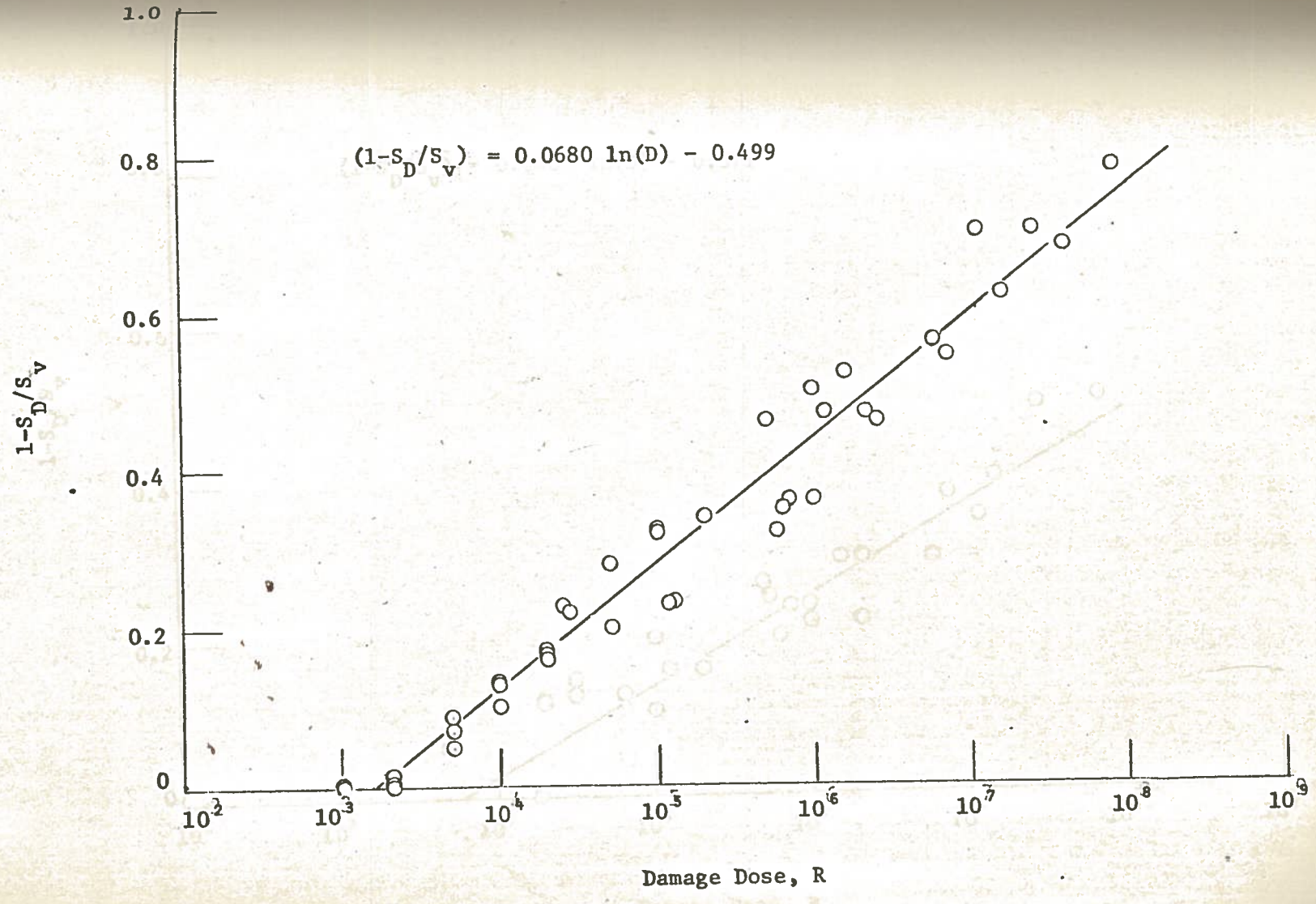

Figure 3-1. Relative Response Versus Damage Dose of Gamma Radiation for 400°C Annealing

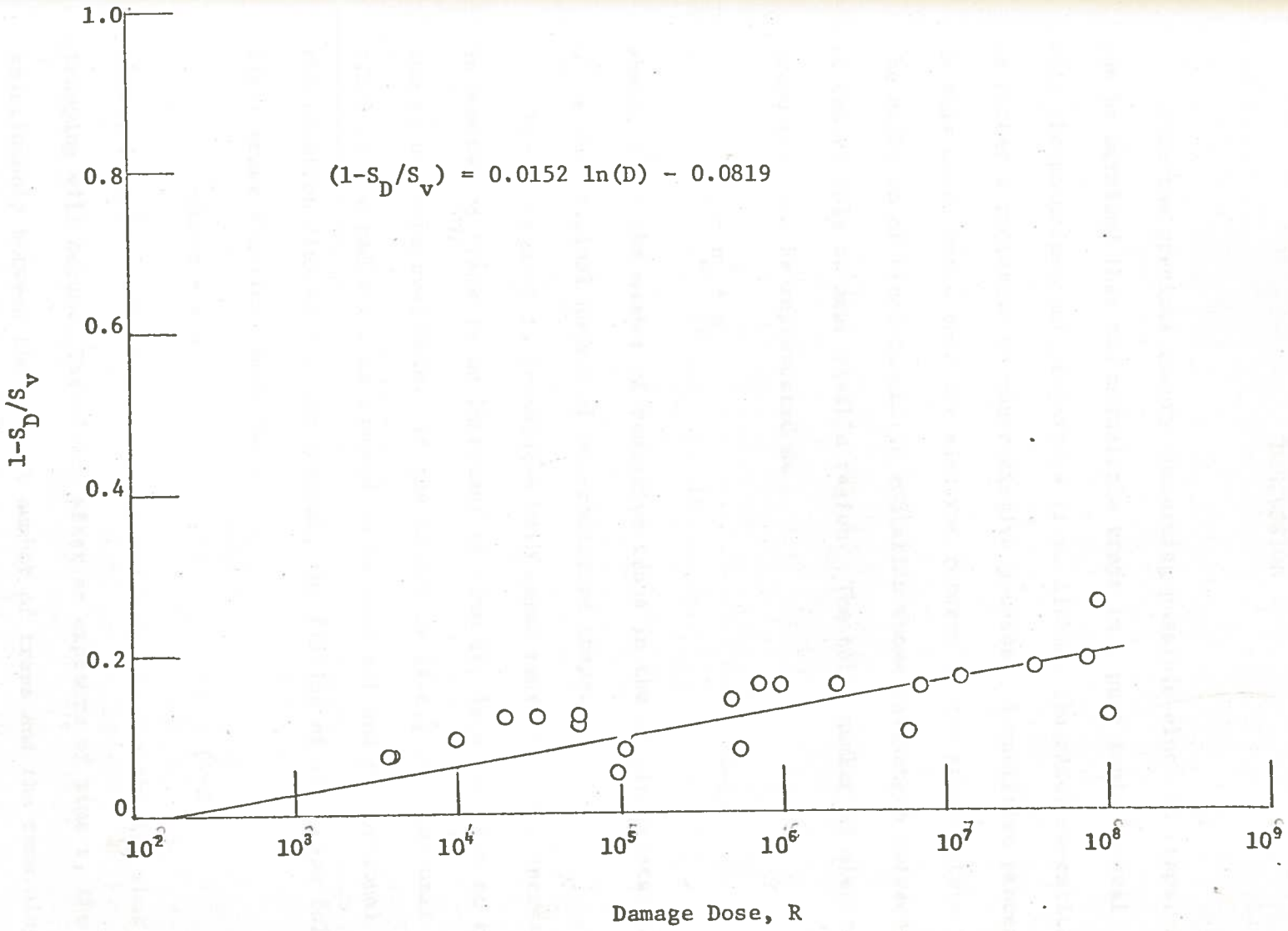

Figure 3-3.. Relative Response Versus Damage Dose of Gamma Radiation for 600°C Annealing

DISCUSSION

From the previous theory concerning possible electron traps, it can be surmised that the metastable traps in a pure ionic crystal with thermoluminescent properties (i.e. lithium fluoride) de-excite by either a radiative or non-radiative process. A radiative process, in this case, means that the electron returns to the ground state with the emission of electromagnetic radiation whose wavelength corresponds to the visible or near visible region. The total number of electron traps can thus be represented as

$$N_o = n_o^* + n_o^\Delta \qquad (4\text{-}1)$$

where, n_o^* is the number of radiative traps in the virgin crystal and n_o^Δ is the original number of non-radiative traps.

When a crystal is irradiated with gamma radiation, the decrease in unoccupied traps in an increment of time dt, is a function of the number of traps available. If the intensity (i.e., dose per unit time) of the radiation is assumed to be constant and proportional to the electron flux within the crystal, the filling of the traps follows first order kinetics, such that,

$$-dn/dt = kIn \qquad (4\text{-}2)$$

where, I is the radiation intensity and k is the probability that trapping will occur. Therefore, after an exposure of time t, the relationship between the initial number of traps and the remaining ones is an exponential function of the form

$$n = n_o e^{-kIt} \qquad (4\text{-}3)$$

It then follows that the number of filled traps is

$$n_f = n_o - n$$

$$= n_o (1-e^{-kE}) \qquad (4-4)$$

where E is the radiation exposure (E=It).

For a particular detection device under reproducible geometry, the response of the virgin crystal is a function of the fraction of the radiative traps available. Assuming a certain constant C which is dependent upon the system, the response is

$$S_v = C \cdot n_f^* / (n_f^* + n_f^\Delta) \qquad (4-5)$$

$$= C \cdot Xn_o^* / (Xn_o^* + Yn_o^\Delta) \qquad (4-6)$$

where

$$X = (1-e^{-k^* E}) \qquad (4-7)$$

and

$$Y = (1-e^{-k^\Delta E}) \qquad (4-8)$$

The distinction is made between k^* and k^Δ because the rate of filling of the radiative and nonradiative traps will more than likely not be the same.

When lithium fluoride is exposed to massive doses of radiation, the defects produced alter the thermoluminescent response, as can be seen from the results plotted in Figures 3-1, 3-2, and 3-3. A logical assumption can then be deduced that the type of traps created are of the non-radiative type which cannot be annealed out at 400°C, such that the fraction of radiative traps is reduced. The total number of

traps in the damaged crystal is then

$$N_D = n_o^* + (n_o^\Delta + n_D^\Delta) \qquad (4\text{-}9)$$

where n_D is the number of newly formed non-radiative traps. Following the same reasoning as before, the response of the damaged LiF is then

$$S_D = C \cdot Xn_o^* / [Xn_o^* + Y(n_o^\Delta + n_D^\Delta)] \qquad (4\text{-}10)$$

The ratio of the response of the virgin crystal as compared to the damaged crystal is therefore

$$R_D \equiv S_v / S_D$$

$$= [Xn_o^* + Y(n_o^\Delta + n_D^\Delta)] / (Xn_o^* + Yn_o^\Delta) \qquad (4\text{-}11)$$

$$= 1 + [Yn_D^\Delta / (Xn_o^* + Yn_o^\Delta) \qquad (4\text{-}12)$$

By letting $Y/(Xn_o^* + Yn_o^\Delta) = B$, equation (8-12) can be written as

$$R_D = 1 + B \cdot n_D^\Delta \qquad (4\text{-}13)$$

which necessitates deriving a dose-dependent expression for n_D^Δ.

The simplest approach for such a problem is to assume that an energetic electron interacts with an ion such that the ensuing vacancy will produce a color center. This is a reasonable assumption because of the reported coloring of the crystals when exposed to very large doses. The most likely target for the electron would be a fluoride ion, such that

$$F^- + e_i \rightsquigarrow F^o + 2e_s^- \qquad (4\text{-}14)$$

where e_i is the incident electron and e_s is a scattered electron. The resulting fluorine atom would probably have sufficient recoil energy to

vacate the lattice position and would be free to migrate in the crystal. If a thermal electron then entered the hole to satisfy the charge deficiency, the result would be the creation of an F center.

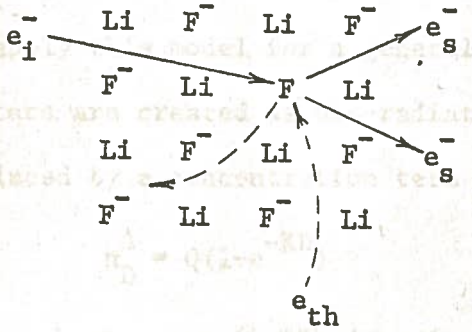

I

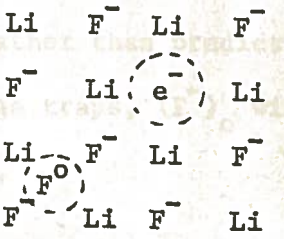

II

The F center would then become a trap for a subsequent calibration-dose exposure. If it is assumed that the F center is a non-radiative trap, then a reduction in thermoluminescence would result because of the competition of the F center with a radiative trap.

Even though the number of fluoride ions is much greater than the gamma-produced electron flux, it is assumed that at large doses the number of available fluoride ions is limited because of lattice distortions and competing reactions. With such an assumption the production of non-radiative traps becomes a matter of first order kinetics. Designating (F^-) as the concentration of available fluoride ions,

$$-d(F^-)/dt = KI(F^-) \qquad (4\text{-}15)$$

Thus for a damage dose of D=It

$$(F^-)_D = (F^-)_o e^{-KD} \qquad (4\text{-}16)$$

The number of non-radiative damage traps produced will be

$$n_D^{\Delta} = (F^-)_o - (F^-)_D \qquad (4\text{-}17)$$

$$= (F^-)_o(1-e^{-KD}) \qquad (4\text{-}18)$$

To apply this model for a general case, rather than predicting F. centers are created as non-radiative damage traps, $(F^-)_o$ will be replaced by a concentration term Q; hence,

$$n_D^{\Delta} = Q(1-e^{-KD}) \qquad (4\text{-}19)$$

Thus substituting (4-19) into (4-13) established the relationship between relative response and damage dose:

$$R_D = 1 + BQ(1-e^{-KD}) \qquad (4\text{-}20)$$

Rearrangement gives

$$(R_D - 1) = BQ(1-e^{-KD}) \qquad (4\text{-}21)$$

which suggests that a plot of (R_D-1) against D should yield a curve with the general shape of a "growth" curve (see Figure 4-1). Further rearrangement gives

$$[(1 + BQ) - R_D] = BQe^{-KD} \qquad (4\text{-}22)$$

which in logarithmic form is

$$\log [(1 + BQ) - R_D] = \log (BQ) - KD \qquad (4\text{-}23)$$

A plot of the quantity on the left against D should result in a straight line with a negative slope.

To test this development against experimental values the relative response $(1-S_v/S_D)$ was converted to R_D for the damaged dosimeters

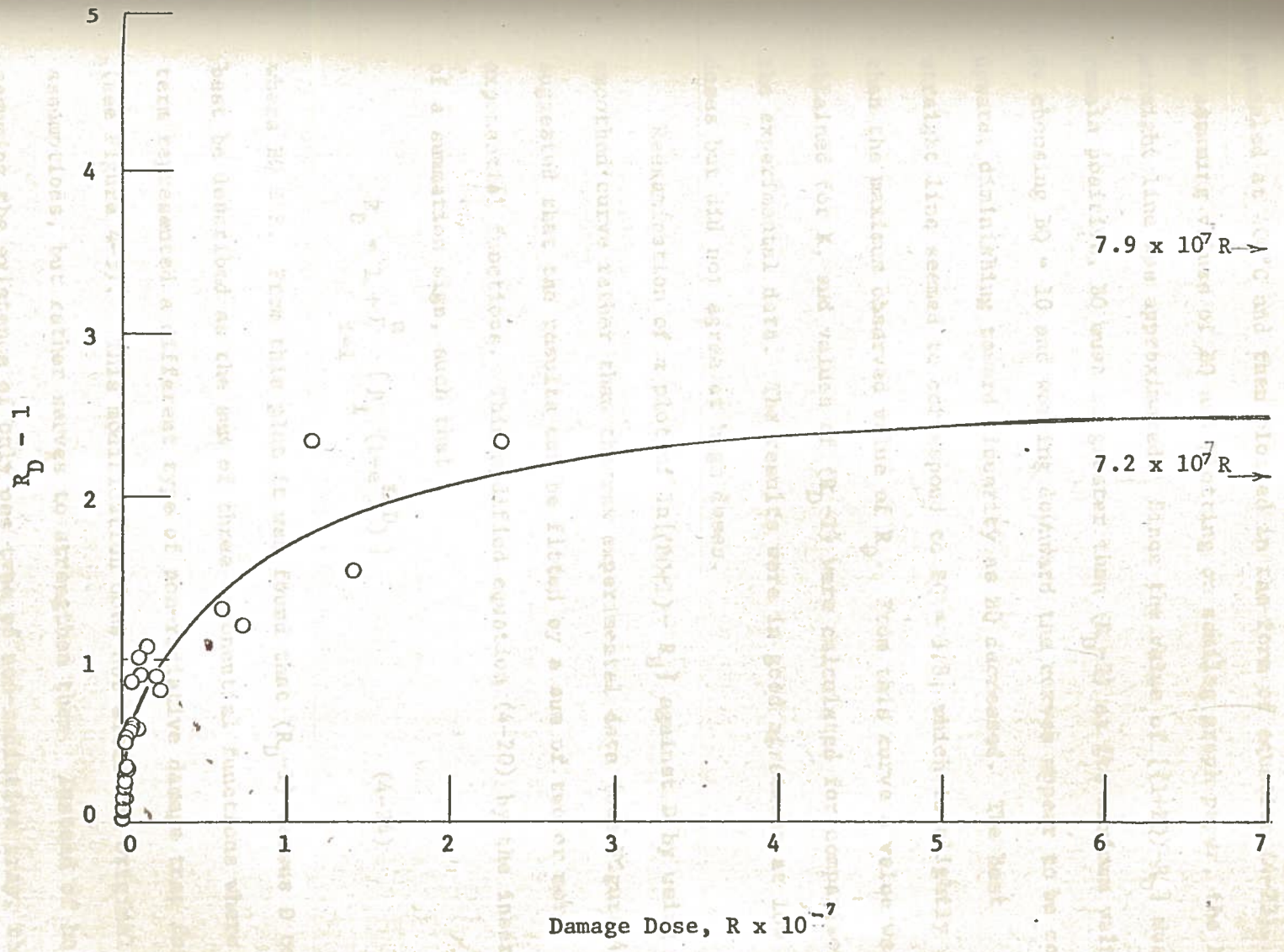

Figure 4-1. "Growth Curve," Linear Plot of Response of Damaged Dosimeter Versus Dose for 400°C Annealing

annealed at 400°C and then plotted in the form of equation (4-23). By assuming values of BQ and plotting on semilog graph paper, the best straight line was approximated. Since the value of $[(1+BQ)-R_D]$ must remain positive, BQ must be greater than (R_D-1) at its maximum value. By choosing BQ = 10 and working downward the curves appear to be concave upward, diminishing toward linearity as BQ decreased. The best straight line seemed to correspond to BQ = 3.8, which is slightly larger than the maximum observed value of R_D. From this curve a value was obtained for K, and values of (R_D-1) were calculated for comparison with the experimental data. The results were in good agreement at low doses but did not agree at high doses.

Reexamination of a plot of $\ln[(BQ+1)-R_D]$ against D by using a smoothed curve rather than the raw experimental data (see Figure 4-2) suggested that the results can be fitted by a sum of two or more exponential functions. This modified equation (4-20) by the insertion of a summation sign, such that

$$R_D = 1 + \sum_{i=1}^{n} [P_i (1-e^{K_i D})] \qquad (4-24)$$

where BQ ≡ P. From this plot it was found that (R_D-1) versus D could best be described as the sum of three exponential functions where each term represented a different type of non-radiative damage trap formation (see Figure 4-3). This modification does not alter the original assumptions, but rather serves to strengthen them. Instead of boldly assuming the existence of only one type of non-radiative trap, there are now three, each being dose dependent. Using the intercepts and slopes obtained from Figure 4-2, the equation which describes the results for

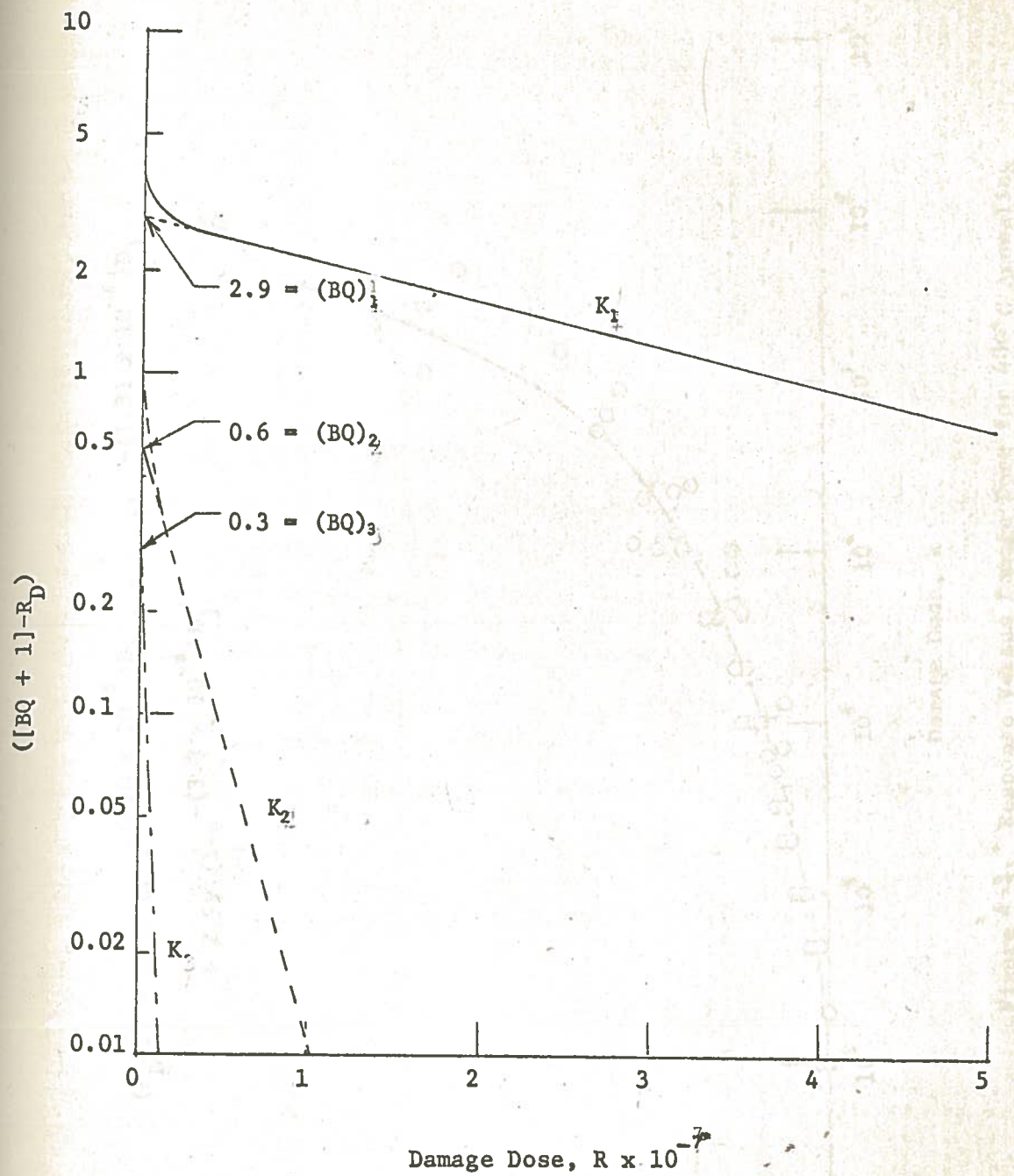

Figure 4-2. Determinations of Constants, BQ, for the Three Types of Traps.

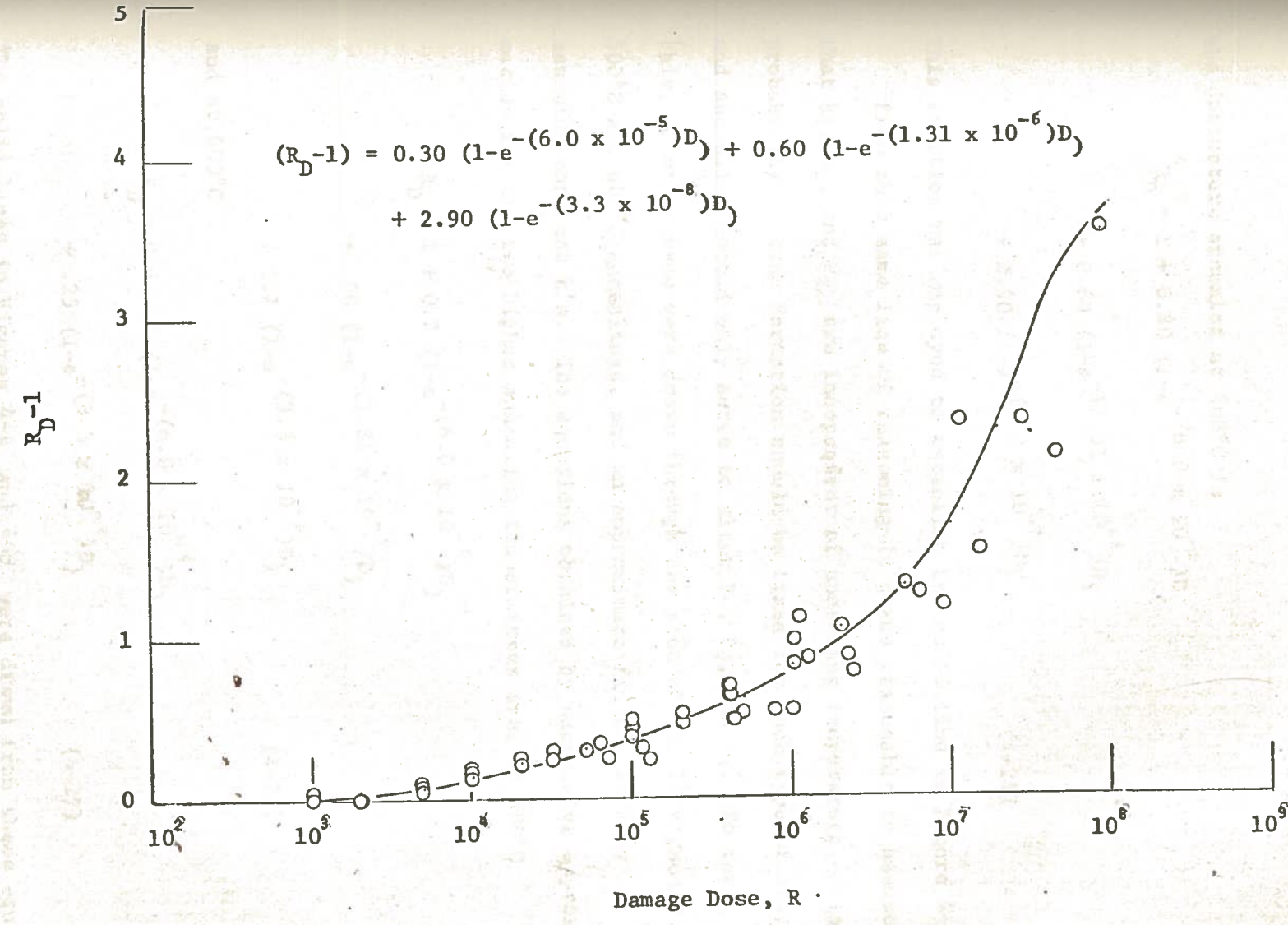

Figure 4-3. Response Versus Damage Dose for 400°C Annealing

the dosimeters annealed at 400°C is

$$R_D = 1 + 0.30\ (1-e^{-(6.0 \times 10^{-5})D}) + 0.60\ (1-e^{-(1.31 \times 10^{-6})D}) + 2.90\ (1-e^{-(3.3 \times 10^{-7})D}) \qquad (4\text{-}25)$$

This equation was employed to establish the solid line in Figure 4-3.

From this same line of reasoning it seems reasonable to assume that k_1, k_2, and k_3 are independent of annealing temperature. The probability of trap formation should be fixed for each type of trap, and annealing should only serve to alter P_1, P_2, and P_3. To test this, smooth curves were drawn through the plot of (R_D-1) versus D for 500°C and 600°C annealings, and an approximate fit was made by assuming constant k's. The equations obtained by successive approximation for the two higher annealing temperatures are, at 500°C

$$R_D = 1 + 0.7\ (1-e^{-(6.0 \times 10^{-5})D}) + .30\ (1-e^{-(1.31 \times 10^{-5})D}) + 1.7\ (1-e^{-(3.3 \times 10^{-8})D}) \qquad (4\text{-}26)$$

and at 600°C

$$R_D = 1 + .20\ (1-e^{-(6.0 \times 10^{-5})D}) + .25\ (1-e^{-(3.3 \times 10^{-8})D}) \qquad (4\text{-}27)$$

The solid lines in Figures 4-4 and 4-5 were drawn from these equations. A plot of P_1, P_2, and P_3 versus annealing temperature (see Figure 4-6),

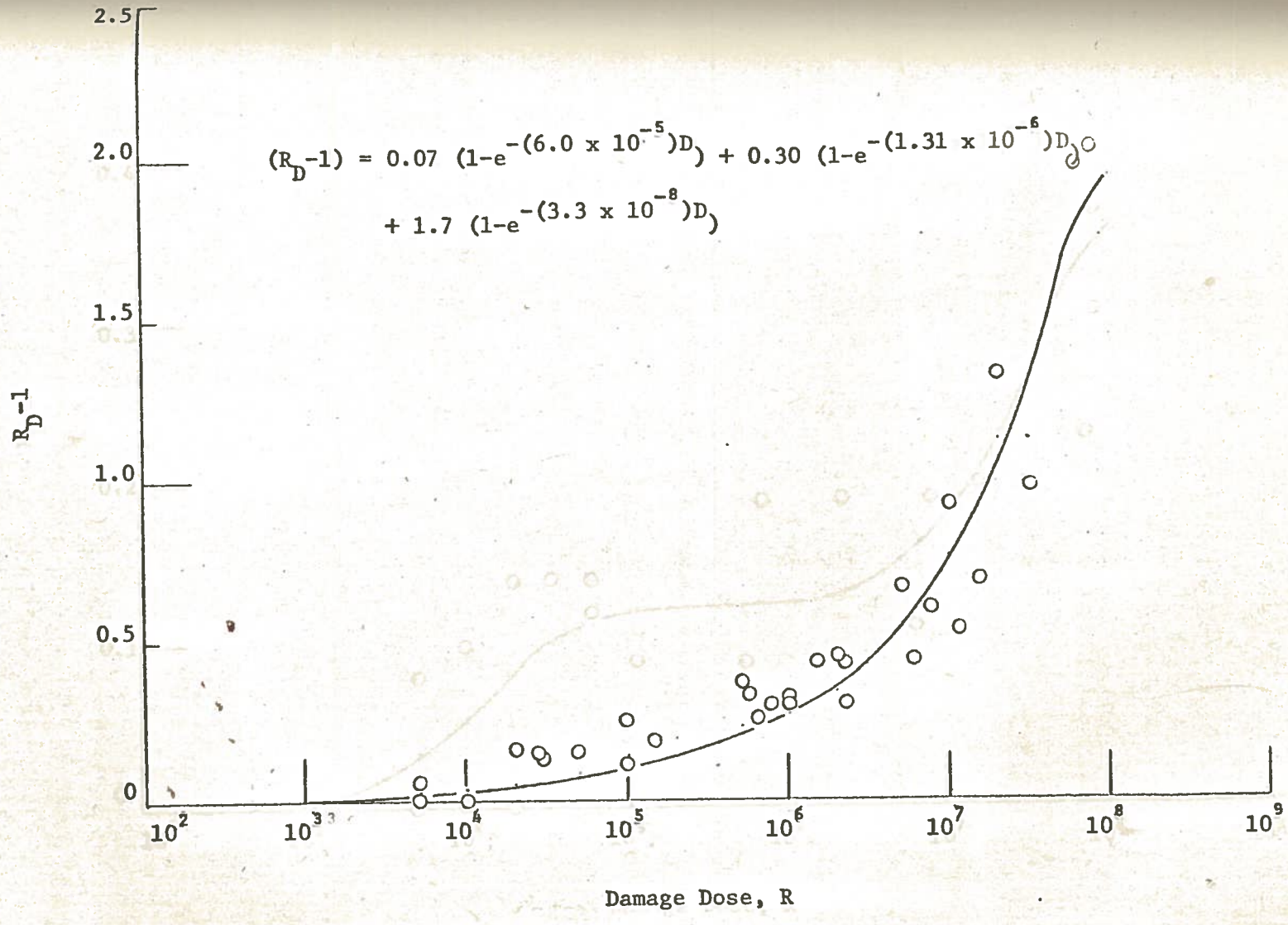

Figure 4-4. Response Versus Damage Dose for 500°C Annealing

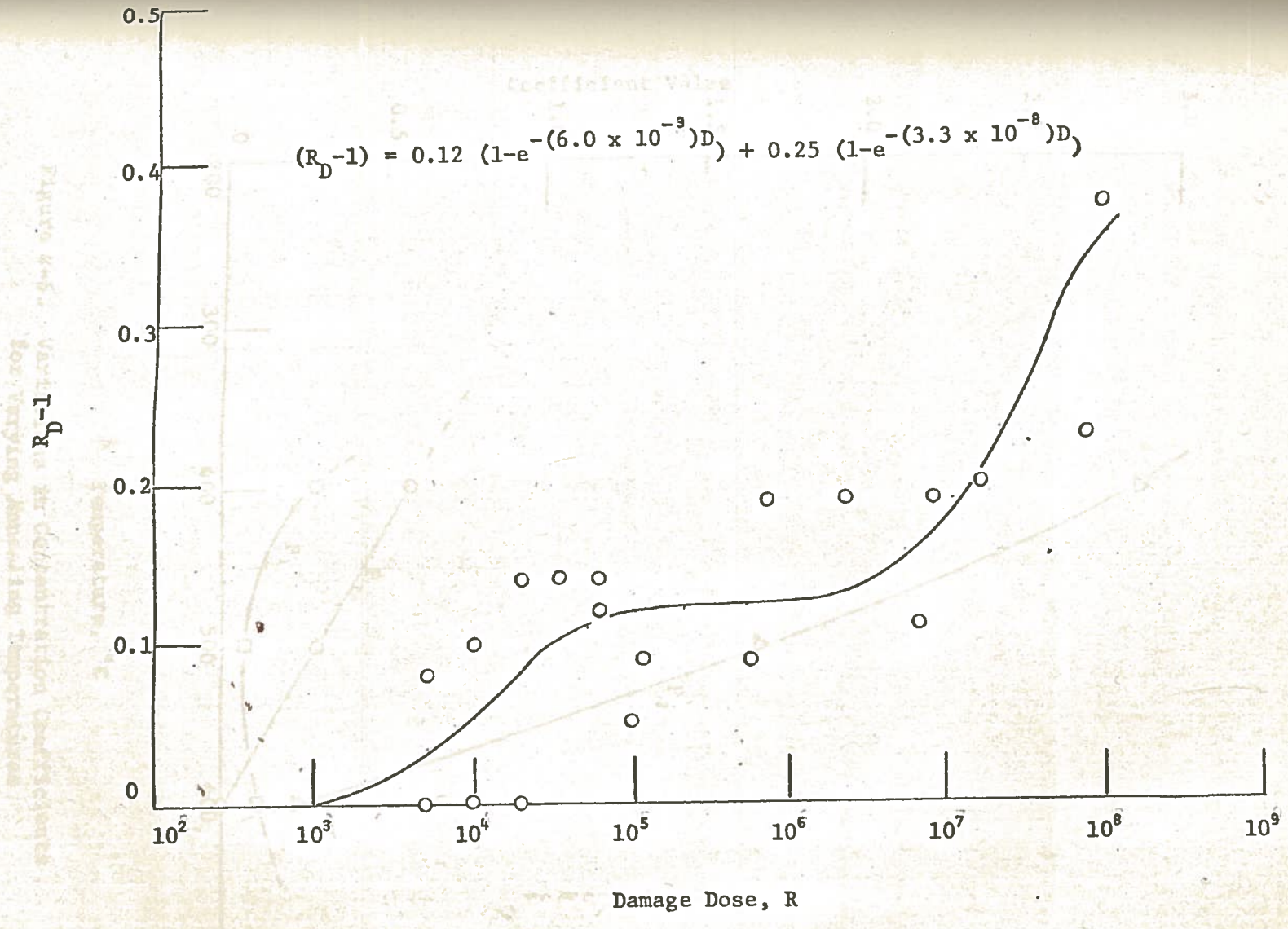

Figure 4-5. Response Versus Damage Dose for 600°C Annealing

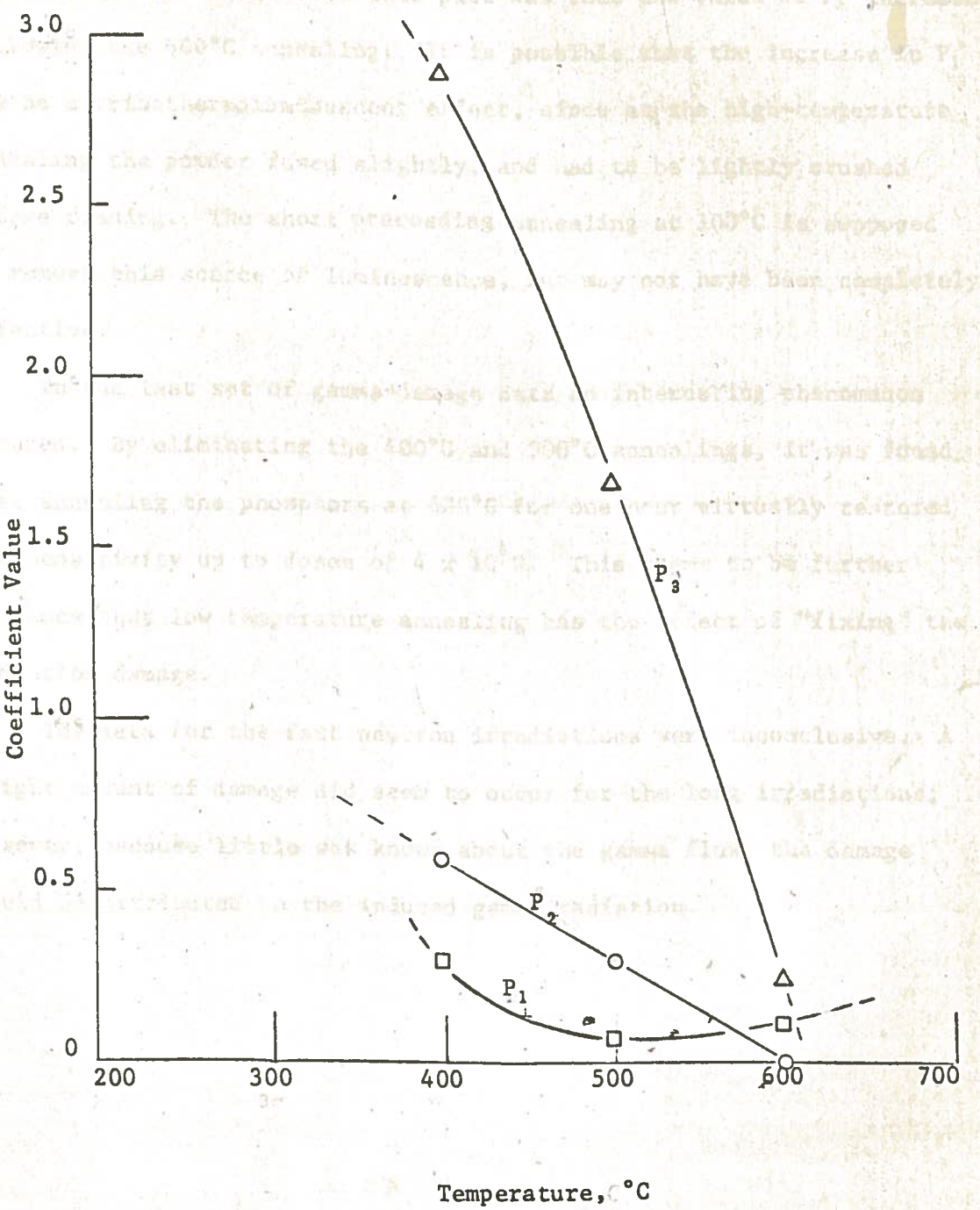

Figure 4-6. Variations in Concentration Coefficients for Varying Annealing Temperatures

however, eliminated any hope of a relationship existing among the P's. The most unusual fact about this plot was that the value of P_1 increased following the 600°C annealing. It is possible that the increase in P_1 may be a tribothermoluminescent effect, since at the high-temperature annealing the powder fused slightly, and had to be lightly crushed before reading. The short prereading annealing at 100°C is supposed to remove this source of luminescence, but may not have been completely effective.

In the last set of gamma-damage data an interesting phenomenon occured. By eliminating the 400°C and 500°C annealings, it was found that annealing the phosphors at 600°C for one hour virtually restored the sensitivity up to doses of 4×10^6 R. This seems to be further evidence that low temperature annealing has the effect of "fixing" the radiation damage.

The data for the fast neutron irradiations were inconclusive. A slight amount of damage did seem to occur for the long irradiations; however, because little was known about the gamma flux, the damage could be attributed to the induced gamma radiation.

SUMMARY AND CONCLUSIONS

The fundamental reasoning behind endeavoring to study radiation damage is to gain some insight as to the mechanisms involved in thermoluminescence.

Thermoluminescence occurs when an electron, which has achieved the excitation energy necessary to reach the conduction band, becomes trapped in a metastable state. When thermal energy is applied to the crystal, the electrons achieve sufficient energy to escape the trap and return to the ground state. The de-excitation mechanism is the release of electromagnetic radiation in the visible or near-visible region. Solid-state physics has explained the existence of various traps caused by lattice defects, and has suggested that thermoluminescence is probably associated with color centers. However, the true nature of the trap is still a matter of speculation.

The research conducted by Marrone and Attix [1] established for gamma radiation damage, the range of doses in which damage occurs; however, no attempt was made to suggest an explanation consisted with the data. Doppke and Cameron [2] reported additional information on gamma damage; however, their doses were too low to extrapolate to the critical range. They suggested that $(1-S_D/S_V)$ can be represented by the sum of two exponentials. All of the literature on neutron damage exposures are not conclusive enough to draw any parallels.

The techniques employed in this research are fairly precise, however, there are many inherent sources of error which place a limit on accuracy. For example, the rapid-transfer mechanism employed reduces

the timing inaccuracies considerably, and the Radocon probe has a ±5% precision.

The standard procedures for annealing the dosimeters were observed before irradiation. The LiF powder was then exposed to damaging doses before annealing them at 400°C again. A uniform dose of 10^3 R was used to compare the response of the damaged powder to that for a control. A similar procedure was followed for 500°C and 600°C annealings.

To correlate experimental data to some theoretical explanation required the formulation of a model for radiation damage. Following Varley [12] and Ehrlich [11], the hypothesis was made that defects induced by the gamma-radiation-created traps de-excite non-radiatively. Thus the fraction of radiative traps available decreases with increasing dose. By assuming first order kinetics for creation of traps

$$(R_D-1) = BQ\ (1-e^{-kD}) \qquad (5-1)$$

where (R_D-1) is a response term, k is a probability of trap creation, D is the dose, and BQ is a trap concentration constant. By assuming that more than one type of competing non-radiative trap is formed equation (5-1) becomes

$$(R_D-1) = \sum_{i=1}^{n} [(BQ)_i\ (1-e^{k_i D})] \qquad (5-2)$$

When this was compared to experimental data for the 400°C annealing, a smooth curve was drawn through the points whose equation was of the type (5-2) where n = 3. Similar procedures were performed on the data for the 500°C and 600°C annealings, assuming that the trapping probabilities k_1, k_2 and k_3 remained constant. As was expected the

general tendency of (BQ) was to decrease with increasing annealing temperatures; however, one value (BQ)$_1$ actually began to increase after the 600°C annealing. This could be a result of tribothermoluminiscence caused by the recrushing of crystals, which had a tendecy to fuse at 600°C. A final set of damaged dosimeters annealed at 600°C without any lower annealings were found to be completely restored in sensitivity up to damaging dose of 4×10^6R. This suggests that low temperature annealings may "fix" radiation damage.

No conclusive evidence can be gleaned from the experimental data on neutron damage.

To extend this problem would first of all require the modifications of technique to reduce the sources of error. To reduce the "fixing" of radiation damage, a logical approach would be to anneal the dosimeters at only one temperature. The successive annealings could have profound effects upon the concentration constants. A close control of the quench to room temperature following annealing should also be maintained.

Probably the most accurate method of determing the types of traps created and destroyed would be to study the absorption spectra before and after irradiations. It is obvious that because each defect exhibits its own particular set of wave functions, the absorption spectra should provide a means of identifying the traps.

BIBLIOGRAPHY

1. M. J. MARRONE and F. H. ATTIX, Health Physics, 10, 431 (1964).

2. K. P. DOPPKE and J. R. CAMERON, Phys. Med. Biol., 11, 624 (1966).

3. B. G. OLTMAN, J. KASTNER, P. TEDESCHI, and J. N. BEGGS; Health Physics, 13, 918 (1967).

4. Amperex Electronic Corporation, "Thermoluminescent Dosimetry," advance edition, (1967).

5. S. GLASSTONE and A. SESONSKE, Nuclear Reactor Engineering, 2nd ed., p. 49-50, D. Van Nostrand Co., Inc., Princeton, New Jersey (1963).

6. LAWRENCE DRESNER, Principles of Radiation Protection Engineering, McGraw-Hill Book Company, Inc., New York, New York (1965).

7. R. W. CHRISTY and A. PYTLE, The Structure of Matter, p. 202-244, W. A. Benjamin, Inc., New York, New York (1965).

8. F. H. ATTIX and W. C. ROESCH, Radiation Dosimetry, 2nd ed., Academic Press, New York, New York (1966).

9. G. J. DIENES and G. H. VINEYARD, Radiation Effects in Solids, Interscience Publishers, Inc., New York, New York (1957).

10. D. S. BILLINGTON and J. H. CRAWFORD, Radiation Damage in Solids, Princeton University Press, Princeton, New Jersey (1961).

11. M. EHRLICH, Health Physics, 12, 1773 (1966).

12. J. H. O. VARLEY, J. Nuclear Energy, 1, 130 (1954); Nature, 174, 886 (1954).

13. R. M. HALL and J. P. LAROCCA, Health Physics, 12, 851 (1966).

14. R. E. SIMPSON, Nuclear Applications, 3, 8, 500 (1967).

15. J. KASTNER, B. G. OLTMAN, and P. TEDESCHI. Health Physics, 12, 1125 (1966).

16. J. R. CAMERON, D. ZIMMERMAN, G. KENNEY, R. BUCH, R. BLAND, and R. GRANT, Health Physics, 10, 25 (1964).

APPENDICES

APPENDIX I

Fundamentals of Thermoluminescence

Gamma interactions with the crystal lattice have the net effect, after a series of complex processes, of promoting electrons from the valence band into the conduction band, and creating excitons

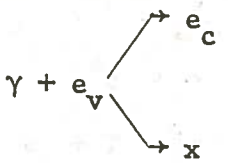

Here, γ is the incident gamma, e_v is a valence-band electron, e_c is a conduction-band electron, and x is an exciton. The rates of formation of these two species can be expressed as

$$\left.\frac{d[e_c]}{dt}\right|_f = k_a I[e_v], \qquad \text{(I-1)}$$

$$\left.\frac{d[x]}{dt}\right|_f = k_b I[e_v], \qquad \text{(I-2)}$$

in which the braces indicate concentrations (e.g., number/unit wt.), I is radiation intensity (e.g., rads/sec), and k_a and k_b are rate constants in appropriate dimensional units. For the purpose of this discussion the rate constants will be assumed to be independent of gamma energy. For a constant dose rate, and assuming that $[e_v]$ is so large that it is never significantly changed, these two equations can be written as psuedo zero-order reactions.

$$\left.\frac{d[e_c]}{dt}\right|_f = k_a' I \qquad \text{(I-3)}$$

$$\left.\frac{d[x]}{dt}\right|_f = k_b' I \qquad \text{(I-4)}$$

Both the exciton electrons and conduction-band electrons have only two ultimate fates: de-excitation to the valence band or capture by a trap

$$e_c \rightarrow e_v + \Delta \qquad \text{(I-5)}$$

$$e_c + T \rightarrow e_T \qquad \text{(I-6)}$$

$$x \rightarrow e_v + \Delta \qquad \text{(I-7)}$$

$$x + T' \rightarrow e_{T'} \qquad \text{(I-8)}$$

The corresponding rate equations are

$$-\left.\frac{d[e_c]}{dt}\right|_d = k_1 [e_c] \qquad \text{(I-9)}$$

$$-\left.\frac{d[e_c]}{dt}\right|_t = \frac{d[e_T]}{dt} = k_2 [e_c][T] \qquad \text{(I-10)}$$

$$-\left.\frac{d[x]}{dt}\right|_d = k_3 [x] \qquad \text{(I-11)}$$

$$-\left.\frac{d[x]}{dt}\right|_T = \frac{d[e_{T'}]}{dt} = k_4 [x][T'] \qquad \text{(I-12)}$$

At steady-state conditions

$$\left.\frac{d[e_c]}{dt}\right|_t = \left.\frac{d[e_c]}{dt}\right|_d + \left.\frac{d[e_c]}{dt}\right|_T \qquad \text{(I-13)}$$

$$\left.\frac{d[x]}{dt}\right|_f = \left.\frac{d[x]}{dt}\right|_d + \left.\frac{d[x]}{dt}\right|_T \qquad \text{(I-14)}$$

Fundamentals of Thermoluminescence - contd.

Hence,

$$k_a' I = k_1 [e_c]_s + k_2 [e_c]_s [T] \qquad \text{(I-15)}$$

$$k_b' I = k_3 [x]_s + k_4 [x]_s [T'] \qquad \text{(I-16)}$$

Then,

$$[e_c]_s = k_a' I / (k_1 + k_2 [T']) \qquad \text{(I-17)}$$

$$[x]_x = k_b' I / (k_3 + k_4 [T']) \qquad \text{(I-18)}$$

Now, if $k_1 >> k_2[T]$, and $k_3 >> k_4[T']$; i.e., the rates of deexcitation are very large and the concentrations of traps are small

$$[e_c]_s \simeq \frac{k_a'}{k_1} I \qquad \text{(I-19)}$$

$$[x]_s \simeq \frac{k_b'}{k_3} I \qquad \text{(I-20)}$$

The rates of trap filling then become

$$\frac{d[e_T]}{dt} \simeq \frac{k_a' k_2}{k_1} I[T] \qquad \text{(I-21)}$$

$$\frac{d[e_{T'}]}{dt} \simeq \frac{k_b' k_4}{k_3} I[T'] \qquad \text{(I-22)}$$

If there is only one kind of trap available, then

$$\frac{d[e_T]}{dt} \simeq \frac{k_a' k_2}{k_1} + \frac{k_b' k_4}{k_3} [T] I \qquad \text{(I-23)}$$

But the rate at which electrons are trapped is equal to the rate at which traps are being filled; hence,

$$-\frac{d[T]}{dt} = \bar{K} I [T] \qquad \text{(I-24)}$$

$$k = Ae^{-E^*/RT}, \qquad \text{(I-29)}$$

in which A and E* are system constants, K is the gas constant, and T is the temperature. Hence

$$-\left.\frac{d[e_T]}{dt}\right|_r = A_r e^{-E_r^*/RT}[e_T] \qquad \text{(I-30)}$$

$$-\left.\frac{d[e_T]}{dt}\right|_{nr} = A_{nr} e^{-E_{nr}^*/RT}[e_T] \qquad \text{(I-31)}$$

But T is a nonlinear function of time, with a generally parabolic shape

$$T \simeq (at + b)^{1/2} \qquad \text{(I-32)}$$

Therefore, the total rate of trap dumping will be

$$\left.\frac{[de_T]}{dt}\right|_{total} = \left.\frac{d[e_T]}{dt}\right|_r + \left.\frac{d[e_T]}{dt}\right|_{nr} \qquad \text{(I-33)}$$

$$= \left[A_r e^{-E_r^*/R\sqrt{at+b}} + A_{nr} e^{-E_{nr}^*/R\sqrt{at+b}}\right][e_T] \qquad \text{(I-34)}$$

APPENDIX II

Tabulated Data

I. Gamma Damage

A. First set of exposures

Damage Dose (R)	Relative Response to 1000 R ($1-S_D/S_V$)		
	400°C annealing	500°C annealing	600°C annealing
0	.00	.00	.00
10^3	.00		
2×10^3	.00		
5×10^3	.07	.06	.07
10^4	.10	[.14]	.09
2×10^4	.17	.14	.12
3.1×10^4	.22	.11	.12
6×10^4	[.06]	.13	.12
1.2×10^5	.23	.16	.08
5.5×10^5	.32	.25	.08
7.2×10^5	.36	.24	.16
10^6	.36	.22	.16
2.2×10^6	.44	.30	.16
7.2×10^6	.54	.38	.16
7.2×10^7	[.57]	.51	.19

B. Second set of exposures

Damage Dose (R)	Relative response to 1000 R ($1-S_D/S_V$)		
	400°C annealing	500°C annealing	600° annealing
0	.00	.00	.00
10^3	.00		
2×10^3	.00		
5×10^3	.05		
10^4	.13		
2×10^4	.18	.14	
3×10^4	.23	.13	
6×10^4	.28		.11
10^5	.32	.20	
5×10^5	.46	.27	.14
6×10^5	.35	.20	[.19]
1.5×10^6	.52	.30	
2.1×10^6	.47	.22	
6×10^6	.56	.30	.10
1.4×10^7	.62	.40	.17
3.6×10^7	.68	.49	.18
7.9×10^7	.78	[.70]	.27

C. Third set of exposures

Damage Dose (R)	Relative Response to 1000 R ($1-S_D/S_V$)		
	400°C annealing	500°C annealing	600°C annealing
0	.00	.00	.00
10^3	.06		
2×10^3	.02		
5×10^3	.09	.00	.00
10^4	.13	.00	.00
2×10^4	.16	.00	.00
5.75×10^4	.20		
10^5	.32	.11	.05
1.15×10^5	.24		
2×10^5	.34	.16	
10^6	.50	.24	.05
1.15×10^6	.47		
1.15×10^7	.70	.35	.06
2.3×10^7	.70		
10^8	[.66]	[.34]	.12

D. Fourth set of exposures

Damage Dose (R)	Relative Response following 600°C annealing
0	.00
10^3	.00
2×10^3	.00
10^4	.00
2×10^4	.00
10^5	.00
2.35×10^5	.00
10^6	.00
4×10^6	.00

II. Neutron Damage

A. Exposures to 14 MeV neutrons

Gamma Dose (R)	Relative response $(1-S_D/S_V)$		
	0 neutron dose	1120 Rad dose	3340 Rad dose
10^3	.00	.04	.09
2×10^3	.00	.06	.05
3×10^3	.00	.02	.04
5×10^3	.00	.01	.08
7×10^3	.00	.00	.05

B. Exposures to 3 MeV neutrons (extruded rods)

Neutron Dose	Relative Response to 1000 R Gamma Dose $(1-S_D/S_V)$
0	.00
870 Rad	.02
1050 Rad	-.01
2300 Rad	-.17

APPENDIX III

Determination of Empirical Formulas

I. 400°C annealing

Dose	ln(D)	[ln(D)]	$(1-S_D S_V)$	$(1-S_D S_V)\ln(D)$
1×10^3	6.908	47.72	0	0
1×10^3	6.908	47.72	0	0
1×10^3	6.908	47.72	0.06	0.4145
2×10^3	7.601	57.77	0.02	0.1520
2×10^3	7.601	57.77	0	0
2×10^3	7.601	57.77	0	0
5×10^3	8.517	72.54	0.07	0.5962
5×10^3	8.517	72.54	0.05	0.4259
5×10^3	8.517	72.54	0.09	0.7665
1×10^4	9.210	84.83	0.13	1.1973
1×10^4	9.210	84.83	0.13	1.1973
1×10^4	9.210	84.83	0.10	0.9210
2×10^4	9.903	98.08	0.17	1.6835
2×10^4	9.903	98.08	0.18	1.7825
2×10^4	9.903	98.08	0.16	1.5845
3×10^4	10.309	106.27	0.23	2.3711
3.1×10^4	10.342	106.05	0.22	2.2757
5.75×10^4	10.960	120.11	0.20	2.1920
6×10^4	11.002	121.05	0.28	3.0806
1×10^5	11.513	132.55	0.32	3.6842
1×10^5	11.513	132.55	0.32	3.6842

Determination of Empirical Formulas - contd.

Dose	ln(D)	$[\ln(D)]^2$	$(1-S_D/S_v)$	$(1-S_D/S_v)\ln(D)$
1.15×10^5	11.653	135.79	0.24	2.7967
1.2×10^5	11.695	136.78	0.23	2.6899
2×10^5	12.206	148.99	0.34	4.1500
5×10^5	13.122	172.20	0.46	6.0361
5.5×10^5	13.218	174.71	0.32	4.2298
6×10^5	13.305	177.01	0.35	4.8553
7.2×10^5	13.487	181.90	0.36	4.6568
1×10^6	13.816	190.87	0.50	6.9080
1×10^6	13.816	190.87	0.36	4.9738
1.15×10^6	13.955	194.75	0.47	6.5589
1.5×10^6	14.241	202.24	0.52	7.3950
2.1×10^6	14.557	211.92	0.47	6.8418
2.2×10^6	14.604	213.28	0.44	6.4257
6×10^6	15.607	243.59	0.56	8.7399
7.2×10^6	15.790	249.31	0.54	8.5266
1.15×10^7	16.258	264.32	0.70	11.3806
1.4×10^7	16.455	270.75	0.62	11.8313
2.3×10^7	16.951	287.34	0.70	11.8657
3.6×10^7	17.399	302.73	0.68	11.8313
7.9×10^7	18.185	330.69	0.78	14.1843
	482.356	6082.34	12.370	173.3566

Determination of Empirical Formulas - contd.

$n = 41$

$\Sigma x = 482.356$

$\Sigma y = 12.370$

$\Sigma x^2 = 6082.34$

$\Sigma xy = 173.2566$

$$\text{slope} = m = \frac{\Sigma x - \Sigma y - n\Sigma xy}{(\Sigma x)^2 - n\Sigma x^2} = \frac{5966.744 - 7103.521}{232667.311 - 249375.940} = 0.0680$$

$$\text{intercept} = b = \frac{\Sigma x^2 \Sigma y - \Sigma x \Sigma xy}{n\Sigma x^2 - (\Sigma x)^2} = \frac{75238.546 - 83571.361}{249375.940 - 232667.311} = -0.499$$

II. 500°C annealing

Dose	ln(D)	$[\ln(D)]^2$	$(1-S_D/S_V)$	$(1-S_D/S_V)\ln(D)$
5×10^3	8.517	72.543	.0	.0
5×10^3	8.517	72.543	.06	.511
10^4	9.210	84.830	.0	.0
2×10^4	9.903	98.079	.14	1.386
2×10^4	9.903	98.079	.14	1.386
3×10^4	10.309	106.275	.13	1.340
3.1×10^4	10.342	106.952	.11	1.376
6×10^4	11.002	121.046	.13	1.430
10^5	11.513	132.547	.20	2.303
10^5	11.513	132.547	.11	1.266
1.2×10^5	11.695	136.779	.16	1.871
2×10^5	12.206	148.988	.16	1.953

Determination of Empirical Formulas - contd.

Dose	ln(D)	$[\ln(D)]^2$	$(1-S_D/S_v)$	$(1-S_D/S_v)\ln(D)$
5×10^5	13.122	172.196	.27	3.543
5.5×10^5	13.218	174.707	.25	3.304
6×10^5	13.205	177.015	.20	2.661
7.2×10^5	13.487	181.899	.24	3.237
10^6	13.816	190.868	.22	3.039
10^6	13.816	190.868	.24	3.316
1.5×10^6	14.221	202.236	.30	4.266
2.1×10^6	14.557	211.919	.22	3.203
2.2×10^6	14.604	213.276	.30	4.381
6×10^6	15.607	243.587	.30	4.682
7.2×10^6	15.790	249.311	.38	6.000
1.15×10^7	16.258	264.318	.35	5.690
1.4×10^7	16.455	270.753	.40	6.582
3.6×10^7	17.399	302.726	.49	8.526
7.2×10^7	18.092	327.327	.51	9.227
	348.377	4684.215	6.01	86.243

$n = 27$

$\Sigma x = 348.377$

$\Sigma y = 6.01$

$\Sigma x^2 = 4684.215$

$\Sigma xy = 86.243$

Determination of Empirical Formulas - contd.

$$\text{slope} = m = \frac{\Sigma x \Sigma y - n\Sigma xy}{(\Sigma x)^2 - n\Sigma x^2} = \frac{2093.746 - 2328.561}{121366.534 - 126473.805} = .0460$$

$$\text{intercept} = b = \frac{\Sigma x^2 \Sigma y - \Sigma x \Sigma xy}{n\Sigma x^2 - (\Sigma x)^2} = \frac{28152.132 - 30045.078}{126473.805 - 121366.534} = -0.371$$

III. 600°C annealing

Dose	ln(D)	$[\ln(D)]^2$	$(1-S_D/S_V)$	$(1-S_D/S_V)\ln(D)$
5×10^3	8.517	72.543	.07	.596
5×10^3	8.517	72.543	.0	.0
10^4	9.210	84.830	.09	.829
10^4	9.210	84.830	.0	.0
2×10^4	9.903	98.079	.12	1.188
2×10^4	9.903	98.079	.0	.0
3.1×10^4	10.342	106.952	.12	1.241
6×10^4	11.002	121.046	.12	1.320
6×10^4	11.002	121.046	.11	1.210
10^5	11.513	132.547	.05	.576
1.2×10^5	11.695	136.779	.08	.936
5×10^5	13.122	172.196	.14	1.837
5.5×10^5	13.218	174.707	.08	1.057
7.2×10^5	13.487	181.899	.16	2.158
10^6	13.815	190.868	.16	2.210
2.2×10^6	14.604	213.276	.16	2.337
6×10^6	15.607	243.587	.10	1.561

Determination of Empirical Formulas - contd.

Dose	ln(D)	$[\ln(n)]^2$	$(1-S_D/S_V)$	$(1-S_D/S_V)\ln(D)$
7.2×10^6	15.790	249.311	.16	2.526
1.4×10^7	16.455	270.753	.17	2.797
3.6×10^7	17.399	302.726	.18	3.132
7.2×10^7	18.092	327.327	.19	3.437
7.9×10^7	18.185	330.693	.27	4.910
10^8	18.420	339.325	.12	2.210
	299.011	4125.939	2.650	38.070

$\Sigma n = 23$

$\Sigma x = 299.011$

$\Sigma y = 2.650$

$\Sigma x^2 = 4125.939$

$\Sigma xy = 38.070$

$$\text{slope} = m = \frac{\Sigma x \Sigma y - n\Sigma xy}{(\Sigma x)^2 - n\Sigma x^2} = \frac{792.379 - 875.610}{89407.578 - 94896.597} = .0152$$

$$\text{intercept} = b = \frac{\Sigma x^2 \Sigma y - \Sigma x \Sigma xy}{n\Sigma x^2 - (\Sigma x)^2} = \frac{10933.738 - 11383.349}{94896.597 - 89407.578} = -.0819$$

VITA

William Wade Ballard Jr. was born in Holden, Louisiana, on September 8, 1944. He received his secondary education at Baton Rouge High School in Baton Rouge, Louisiana, from which he graduated in May, 1962. In September of that year he enrolled in Louisiana State University, Baton Rouge, Louisiana. The Bachelor of Science Degree in Mechanical Engineering was granted to him in January, 1967. Upon graduation, he enrolled in the Graduate School of Louisiana State University and is now a candidate for the Master of Science Degree in Nuclear Engineering in August, 1968.